Environmental Science: Atmospheres

ROYAL SOCIETY OF CHEMISTRY

PAPER

View Article Online
View Journal | View Issue

Cite this: *Environ. Sci.: Atmos.*, 2025, **5**, 110

Aerosol and precipitation composition at a coastal New England site (Acadia National Park): implications for air quality and aerosol composition during cold air outbreaks†

Addison Seckar-Martinez,[a] Grace Betito,[b] Lakshmi Parakkat[b] and Armin Sorooshian *[ab]

This study investigates aerosol and wet deposition chemistry at Acadia National Park (Maine, U.S.) using data between 1 January 2001 and 31 December 2021. Results show that $PM_{2.5}$ is highest in summer and dominated by sulfate salts and organics (less contribution from elemental carbon), whereas nitrate salts and sea salt were highest in winter. Fine soil is most pronounced from March through August due most likely to long-range transport. Residual mass ($PM_{2.5}$ – reconstructed $PM_{2.5}$) was negative from November–March, with reasons discussed for its seasonal changes. Major regional sources of pollution are upwind from populated cities generally to the southwest of Acadia. Extreme $PM_{2.5}$ events are mostly driven by regional pollution events with others due to transported summertime biomass burning plumes that increased in frequency in the most recent years. Aerosol composition on cold air outbreak days showed that ammonium sulfate and organics dominated $PM_{2.5}$, which provides useful information for studies focused on understanding the formation and evolution of offshore cloud decks during the winter. Monthly mean pH in wet deposition ranges from 4.8 to 5.1 with the lowest values in July when contributions from acidic ions are highest (sulfate, nitrate). Average annual pH increased from 4.64 to 5.23 over the study period coincident with reductions in sulfate and nitrate levels. Sea salt constituents dominated the wet deposition aqueous ion concentrations from November to March, whereas in the other months sulfate and nitrate were highest. Interrelationships between aerosol and wet deposition species relevant to secondarily produced species, dust, and sea salt provide support for aerosol–precipitation interactions that warrant a further look with more robust methods.

Received 21st August 2024
Accepted 19th November 2024

DOI: 10.1039/d4ea00119b

rsc.li/esatmospheres

Environmental significance

Air quality at coastal sites is important for the public welfare of many living in these areas globally. Coastal aerosol properties also have implications for cloud properties offshore along with ocean biogeochemistry owing to wet deposition. This study reports on co-located measurements of aerosol and wet deposition composition at Acadia National Park (Maine, U.S.). The relative influence of aerosol type (*i.e.*, sulfate/nitrate, organics, dust, salt, smoke) varies depending on time of year due to influence of meteorology and transport patterns, with regulatory actions having shown success since 2001 in reducing levels of sulfates and increasing wet deposition pH. Results reveal the importance of sulfate and organics in the winter, including during cold air outbreaks. Correlations between aerosol and wet deposition species motivate future work into aerosol–precipitation interactions in more robust ways.

1 Introduction

Coastal areas are not only home to many of the world's most populated cities but they are important sources of pollution impacting downwind marine regions with implications for clouds, climate, and biogeochemical cycles. Owing to the difficulty of conducting routine long-term sampling of air quality variables over the ocean, coastal sites are critical to assess air pollution characteristics affecting populated coastal cities along with providing insight into air mass properties advecting offshore. Aerosol advected offshore can impact cloud formation and evolution. This is especially important for coastal sites adjacent to the northwest Atlantic due to persistent continental outflow and the high uncertainties associated with aerosol–cloud interactions in this region having a broad range of cloud types across the year.[1–6] Of particular interest in this study is the composition of wintertime aerosol advected offshore due to the

[a]*Department of Chemical and Environmental Engineering, University of Arizona, Tucson, AZ, 85721, USA. E-mail: armin@arizona.edu*

[b]*Department of Hydrology and Atmospheric Sciences, University of Arizona, Tucson, AZ, 85721, USA*

† Electronic supplementary information (ESI) available. See DOI: https://doi.org/10.1039/d4ea00119b

higher cloud fractions at that time of year over the northwest Atlantic.[3] Especially important are cold air outbreaks (CAOs) that are most common in winter months giving rise to complex cloud systems that transition from overcast clouds (typically organized into roll-like patterns) into open-cell cloud fields with lower cloud fraction (see Fig. 1) and thus reduced overall reflective properties.[7–13] These systems arise when cold air advects over the warm ocean surface, especially over the Gulf Stream, resulting in strong heat fluxes that give rise to these overcast clouds that can contain both liquid droplets and ice.[14] One aspect of better understanding the life cycle and nature of clouds comprised of both liquid and ice in CAOs is knowing more about particles upwind of the cloud decks that can serve as the cloud condensation nuclei (CCN) and ice nuclei (IN).[15] Reduced cloud fractions in other seasons of the year[3] do not diminish the importance of characterizing the composition of aerosols advected offshore that can impact a range of cloud types from stratiform to deeper cumulus clouds.[16–18] Interactions between aerosols and clouds are linked to the largest uncertainty in estimates of total anthropogenic radiative forcing.[19]

The U.S. East Coast has many populated coastal cities but they become less populous to the far northeastern parts closer to Maine by the U.S.-Canada border. Past work focused on the U.S. East Coast has shown that both particulate matter with aerodynamic diameter less than 2.5 μm ($PM_{2.5}$) and total wet deposition ionic concentrations are lowest in Maine and generally increase (more clear for $PM_{2.5}$) moving farther south towards Florida.[20] The focus of this work is a coastal site in Maine (Acadia National Park), which is impacted by transport from nearby states to the southwest with more urban and industrial emissions, and also influenced by long-range transport such as with Asian dust[21,22] and biomass burning from western part of North America and even Siberia.[23–25] A previous study examining Acadia NP and other sites in Vermont and Washington D.C. suggested that secondary organic aerosol (SOA) is generally underpredicted over the northeast U.S.[26] warranting more attention to composition characteristics.

There have been very limited air quality based studies for the coastal parts of Maine, with other reports available from nearby states such as New Hampshire where it is documented that low and high $PM_{2.5}$ generally coincide with air coming from north/northwest and south/southwest, respectively.[27] A ship cruise across the Gulf of Maine revealed that major aerosol types were sourced from local and regional areas (*e.g.*, northeast U.S. urban corridor including New York and Boston), and long range sources such as the U.S. Midwest and wildfires from western parts of North America.[28] That[28] and other work[29] have also showed the importance of organic matter, which was the dominant component of the submicrometer aerosol mass over the Gulf of Maine. A number of studies at Appledore Island off the coast of Maine focused on inorganic bromine and chlorine,[30] nitric acid phase partitioning,[31] and lifecycle characteristics of ammonia.[32] However, knowledge gaps from the aforementioned studies include a long-term view of PM and wet deposition chemistry, including especially examining interrelationships between species among the two types of datasets.

The aim of this study is to take advantage of co-located aerosol and wet deposition monitoring data over a long-term period at Acadia National Park (Maine, U.S.) to characterize chemical attributes throughout an annual cycle and across 21 years, along with exploring interrelationships between aerosol and wet deposition chemistry. This work builds on previous studies intercomparing these two types of datasets to better characterize atmospheric composition and to indirectly gain insights into potential interrelationships between particles and

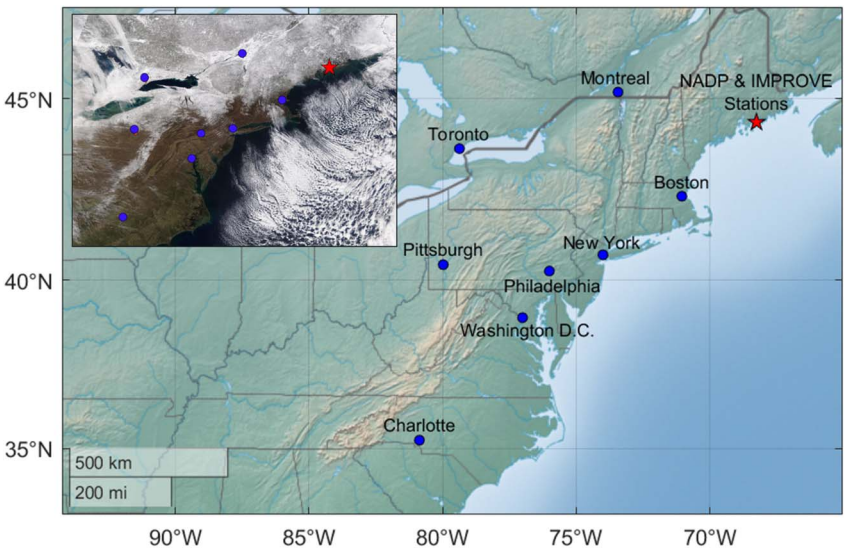

Fig. 1 Map of the northeast U.S. depicting with a red star the location of the Interagency Monitoring of Protected Visual Environments (IMPROVE) and National Atmospheric Deposition Program (NADP) stations co-located in Acadia National Park, Maine (Image Source: Google Earth). Shown for context with blue markers are selected major cities in the U.S. and Canada. The inset map shows the same locations but overlaid on MODIS visible imagery from NASA Worldview from 1 March 2020, which coincided with a cold air outbreak as demonstrated with the classical cloud streets that are typical for these events.

clouds[33–35] since the composition of precipitation is impacted by aerosol particles that seed the droplets in the first place or that may be scavenged by precipitation drops. More specifically, rainout (*i.e.*, in-cloud scavenging) is the process by which species are removed from cloud *via* falling drops whereas washout (*i.e.*, below-cloud scavenging) is when species are removed in air below cloud bases due to being collected by precipitating rain drops. We caution that the datasets used cannot distinguish between the relative importance of those forms of scavenging. The structure of this paper is as follows: Section 2 provides an overview of datasets and methods; Section 3 provides a detailed characterization of aerosol composition with special focus on extreme $PM_{2.5}$ events and aerosol composition during CAOs, followed by results for precipitation composition, and then interrelationships between the two datasets; and Section 4 provides conclusions.

From the outset we note that among the objectives of this study, one is not to investigate aerosol–cloud interactions directly but to learn from possible relationships between species in co-located aerosol and wet deposition measurements to motivate targeted future studies examining such interactions with datasets more robust for such research including airborne measurements. Also, due to the growing interest in CAOs over the northwest Atlantic,[12,36–40] the results of the aerosol composition analysis during those periods at Acadia NP are potentially useful for other studies needing some frame of reference of what aerosol composition is like during these events at a coastal site upwind of where cloud decks form over the northwest Atlantic (Fig. 1).

2 Methods

2.1 Site description

This work focuses on Acadia National Park (Fig. 1) located in the northeast U.S., ~100 km from the U.S.-Canada border and along the coast of the northwest Atlantic Ocean. The population of the surrounding area, Hancock, Maine, is approximately 57 000.[41] Acadia NP is known for the scenic trails through the mountains along the ocean shoreline and is most populated in the summer months (June to September).[42] This coastal site is a Class 1 area as designated by the Environmental Protection Agency (EPA), meaning that it is of the higher environmental quality and requires maximum protection. The site is downwind of major urban and industrial areas to the west and southwest (*e.g.*, New York, Boston (Massachusetts), Philadelphia/Pittsburgh (Pennsylvania), Washington D.C., Montreal and Toronto in Canada), with the added influence at times from air masses moving onshore from the northwest Atlantic. An added source of pollution includes long-range transport of aerosol types such as smoke and dust.[22,23]

2.2 IMPROVE aerosol composition

The IMPROVE site at Acadia NP (Fig. 1) has the following geographic details: latitude = 44.3771; longitude = −68.261; elevation = 157.333 m. Aerosol data are obtained from the Interagency Monitoring of Protected Visual Environments (IMPROVE[43]) database, accessed from the Federal Land Manager Environmental Database (**http://views.cira.colostate.edu/fed/**). IMPROVE monitors and collects air composition data for a 24 h period every third day. Samplers have four modules that collect various components that contribute to aerosol particles at each IMPROVE station. Once the samples are collected, they are analyzed at a central laboratory, and the data are sent to the EPA Air Quality System database. In addition to gravimetric mass of total $PM_{2.5}$ and PM_{10} (difference of PM_{10} − $PM_{2.5}$ being PM_{coarse}), the major components for the $PM_{2.5}$ fraction used in this study include NH_4NO_3, $(NH_4)_2SO_4$, sea salt, fine soil, organic matter, and elemental carbon (EC). The aforementioned $PM_{2.5}$ constituents are derived based on the method of ref. 44 and are referred to as the reconstructed fine mass (RCFM) components of $PM_{2.5}$ mass. We note that fine soil is interchangeable with fine dust in the literature and accounts for mineral particles.[45] The difference between the gravimetric $PM_{2.5}$ and total RCFM mass is often referred to as the residual. Further details about IMPROVE data quality are provided elsewhere[46,47] along with data usage details.[48] Data are used for Acadia NP over a 21 year period from 1 January 2001 to 31 December 2021.

2.3 NADP wet deposition composition

The National Atmospheric Deposition Program (NADP; **http://nadp.slh.wisc.edu/ntn/**) collects precipitation samples at sites across the U.S., with the one of interest in this work being co-located with the IMPROVE aerosol monitoring station in Acadia NP. NADP precipitation samples are collected for a seven day period on every Tuesday morning. The collecting device detects when precipitation is falling to ensure wet-only-sampling for accurate results. The collected precipitation is analyzed for ions including ammonium (NH_4^+), sulfate (SO_4^{2-}), nitrate (NO_3^-), chloride (Cl^-), bromide (Br^-), potassium (K^+), magnesium (Mg^{2+}), and sodium (Na^+). pH is used in this study as an indicator of the acidity of the rain, and was measured using a standard pH meter (Mettler S700) supplied by the Central Analytical Laboratory (CAL). The methodology involved measurements in vials after confirmation that samples were free of contamination. The pH of each sample is determined by analysis of free acidity based on the hydrogen ion (H^+) concentration. All of the aforementioned chemical measurements are quality assured by the CAL.

2.4 Meteorological data

Meteorological data at Acadia NP for temperature, relativity humidity, wind speed, and solar radiation are obtained from the National Park Service based on data collected at the McFarland Hill site in Acadia NP (**https://ard-request.air-resource.com/data.aspx**). Accumulated precipitation data are obtained from the NADP database (**https://views.cira.colostate.edu/fed/Pub/DatasetDetail.aspx?dsidse=5201**). Planetary boundary layer height (PBLH) data are obtained from the Modern Era-Retrospective Analysis for

Research and Applications (MERRA-2) at a spatial resolution of 0.5° × 0.625°.[49]

The National Park Service records data every hour for temperature (°C), relative humidity (%), wind speed (m s^{-1}), wind direction, and solar radiation (W m^{-2}). The monthly mean is calculated for each parameter using data from January 2001 to December 2021, whereas the monthly mode value is obtained for wind direction. NADP collects weekly data for precipitation (mm), which are used to calculate the monthly accumulated precipitation. MERRA-2 provides the mean monthly planetary boundary layer height (m), which is then averaged to compute the monthly average for the study's time range.

2.5 Concentration weighted trajectories

A subset of results below show the trajectory paths leading to the highest $PM_{2.5}$ levels at Acadia NP using IMPROVE data combined with back-trajectory results computed with the NOAA Hybrid Single-Particle Lagrangian Integrated Trajectory (HYSPLIT) model.[50,51] The HYSPLIT model was run using the following options: (i) four days for back-trajectory duration for five years (January 2017 to December 2021); (ii) trajectories generated four times per day (00, 06, 12, 18 UTC); (iii) ending altitude of 500 m above ground level (AGL) at Acadia NP; (iv) Global Data Assimilation System (GDAS) data at 1° resolution; (v) "model vertical velocity" method. While the GDAS data have coarse resolution, they are deemed suitable for this study where only general paths are desired, as done in other works.[52] Also, the ending altitude of 500 m AGL is often used in studies of this nature trying to explain characteristics of surface air quality.[53–55]

The concentration-weighted trajectory (CWT) results are based on using the IMPROVE $PM_{2.5}$ data to assign a weighted concentration to a spatial grid cell of 0.5° × 0.5° dimension. More specifically, each cell is assigned a mean of sample concentrations corresponding to trajectories passing through that same cell using the following relationship:

$$C_{ij} = \frac{1}{\sum_{l=1}^{M} \tau_{ijl}} \sum_{l=1}^{M} c_l \tau_{ijl} \quad (1)$$

where C_{ij} is the weighted mean concentration in the ijth cell, l is the trajectory index number, M represents the number of total trajectories, C_l is the measured concentration at the arrival point (Acadia NP) for trajectory l, and τ_{ijl} signifies time spent by trajectory l in the ijth cell. The reader is referred to past works for more details about CWT if interested.[56,57] Our examination of data for 2017–2021 for the CWT analysis is believed to be representative of the full study duration of 2001–2021.

2.6 Extreme aerosol event analysis

In previous studies, extreme aerosol events have been defined as days when the mass of a given parameter exceeds a certain threshold, such as over the 90th percentile.[53,58] In this study, the criteria for an extreme aerosol event is established to highlight the most polluted days at Acadia NP. An extreme event is defined as a day in which the $PM_{2.5}$ concentration is ≥98th percentile for each given month from January 2002 to December 2006 and separately also for January 2017–December 2021. The reason two sets of years were analyzed is that $PM_{2.5}$ reductions have occurred between 2002 and 2021 (shown later), which would bias the results such that most extreme events would be in the first few years; examining instead the first and last few years separately provides a snapshot of how the extreme event characteristics changed during the study duration. For those days we examine IMPROVE data in combination with aerosol type information from the Navy Aerosol Analysis and Prediction (NAAPS) system. NAAPS provides data for the transportation of sulfate, dust, and smoke[59] and is found at **https://www.nrlmry.navy.mil/aerosol/**. As the web repository does not have a complete set of imagery for 2001, we start the extreme event analysis in 2002 rather than 2001. The surface mass concentrations and aerosol optical depth (AOD) of each component are recorded every six hours and presented at a spatial resolution of 1° × 1°. The data from NAAPS are used for the identified extreme aerosol events to categorize them as having had strong influence from sulfate, dust, and/or smoke.

2.7 Criteria for cold air outbreaks

As motivated in Section 1, this study takes a special look at aerosol composition on very cold days typically coinciding with cold air outbreaks (CAOs) during the winter. To identify these cases, we used a number of datasets including imagery from NASA Worldview (**https://worldview.earthdata.nasa.gov**) and meteorological data from the National Park Service. We focused on the months of December, January, February, and March from 2016 to 2021 as these tend to be months with a high frequency of CAOs over the northwest Atlantic.[3,11,16] For each day in the time range, Moderate Resolution Imaging Spectroradiometer (MODIS) visible imagery data from NASA Worldview is used to identify "cloud streets", which are typical of CAOs.[6,60] An example of such an event from 1 March 2020 for a CAO studied in previous research[12,39,61] is illustrated in Fig. 1; this event shows how the Acadia NP site is directly upwind of the formation of cloud streets that are advected towards the southeast. However, detection of these features can be challenging if there are multiple cloud layers with higher ones interfering with identification of cloud streets closer to the ocean surface. From those CAO events identified successfully, the daily mean values for temperature, relative humidity, wind speed, and accumulated precipitation on those particular full days were obtained. The statistics for these variables on CAO days confirmed with MODIS visible imagery were compared to all other days in the same months (December–March) when IMPROVE data were available. Temperature showed the clearest difference (detailed results shown later), with median values of −8.57 °C and −0.79 °C for CAO and non-CAO days, respectively. This helped to support the identification of the CAO days.

IMPROVE composition data were then compared between CAO and non-CAO days for December through March between 2016–2021. The more abbreviated time duration examined was meant to be more representative of current conditions coinciding with recent aerosol–cloud interaction studies over the

northwest Atlantic sampling during CAOs like the NASA Aerosol Cloud meTeorology Interactions oVer the western ATlantic Experiment.[1] We specifically use PM_{coarse}, $PM_{2.5}$, and the mass concentrations and relative mass fractions of the RCFM components of $PM_{2.5}$ (ammonium nitrate, elemental carbon, sea salt, ammonium sulfate, organic mass, fine soil). NADP data were not used in this analysis as they had weekly time resolution and could not be matched onto individual days with CAO events.

2.8 Calculations and limitations

One aspect of this study is to intercompare data from the NADP and IMPROVE measurements as done in past works.[33–35] Time synchronization of the two datasets is necessary to compare aerosol data with precipitation data. For each value provided by NADP, an average value from IMPROVE was computed for each week. Once a weekly value is assigned from each database in the study period, correlation coefficients (r) could be calculated between IMPROVE and NADP variables with statistical significance (*i.e.*, p-value <0.05) determined using a two-tailed Student's t-test.

If significant relationships emerge between the aerosol and wet deposition composition variables, two possibilities are noteworthy that are relevant to aerosol–precipitation interactions: (i) the composition of aerosol at the IMPROVE site is representative of the aerosol and/or trace gases that contributed to cloud droplets that eventually grew to sizes sufficiently large to fall as precipitation; and (ii) the falling precipitation scavenged the aerosol and/or trace gases[62] that were influential as well at the surface IMPROVE site. We caution that this type of analysis cannot prove causality and there are challenges with unambiguously connecting surface level aerosol with precipitation falling at the same location. An obvious limitation of this method is that the composition of the wet deposition may have little to do with the surface aerosol characterized by the IMPROVE site owing to a different air mass with varying composition influencing the clouds producing the measured wet deposition. If strong correlations are observed pointing to either of the two explanations above, this at least motivates continued research to find more evidence. We are interested in possible relationships to motivate future work as it relates to the parts of this study focused on intercomparing IMPROVE and NADP data.

3 Results and discussions

3.1 Meteorological profile

Prior to examining aerosol and wet deposition chemistry, we provide a summary of the meteorology using monthly mean (mode for wind direction) values at Acadia NP based on data over the 21 year period examined (Fig. 2). Incident solar radiation expectedly followed the trend of temperature, both of which were highest in the summer (June–August) with temperature peaking in August (17.7 °C) and being lowest in wintertime with a minimum in January (−8.9 °C). Solar radiation had a peak in July (231.3 W m^{-2}) and a minimum value in December (23.21 W m^{-2}). Relative humidity did not exhibit a wide range throughout the year, with the minimum being in March (67.1%) and maximum in December (77.7%). High wind speeds were detected in the spring months (March–May) with a peak in April (3.5 m s^{-1}) and the minimum in August (2.5 m s^{-1}). Winds were typically from the southwest based on monthly mode values, ranging from 229° (April, June) to 243° (January). Fig. S1† additionally shows wind rose plots for each

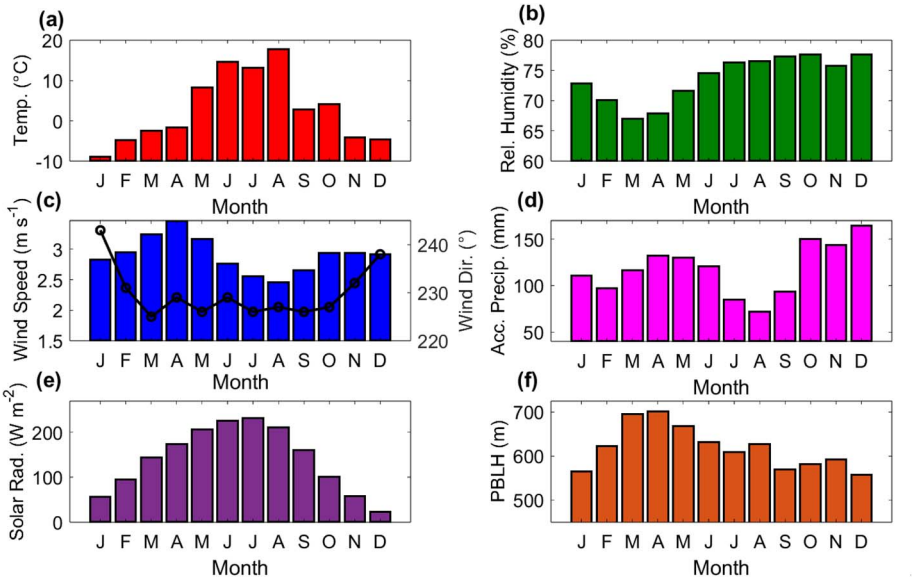

Fig. 2 Monthly mean (mode for wind direction) values based on data from January 2001–December 2021 at Acadia NP (Maine) for (a) temperature (National Park Service, NPS), (b) relative humidity (NPS), (c) wind speed (left y-axis and blue bars) and scalar wind direction (right y-axis and black markers) (NPS), (d) accumulated precipitation (NADP), (e) solar radiation (NPS), and (f) planetary boundary layer height (MERRA-2). Note that accumulated precipitation monthly values represent the average monthly sum for a given month of a year across the 21 years.

season summarizing how winds typically range from the southwest to the west with some influence extending from the northwest to the northeast. Accumulated precipitation exhibited a bimodal profile with peaks in April (132.5 mm) and December (164.6 mm), and a minimum in August (71.9 mm). PBLH was most similar to wind speed's annual profile, with highest values in the spring months, peaking in April (~700 m).

3.2 Aerosol profile

Monthly mean values of $PM_{2.5}$, PM_{10}, and $PM_{2.5}:PM_{10}$ are summarized in Fig. 3a. The $PM_{2.5}:PM_{10}$ ratio provides insight into when local sources of coarse aerosol are relatively more influential (*i.e.*, lower ratios).[63] Both $PM_{2.5}$ and PM_{10} reach their highest levels in the summer months of June–August, similar to ambient temperature and solar radiation. The maximum values of $PM_{2.5}$ and PM_{10} occurred in July with values of 6.4 μg m^{-3} and 9.15 μg m^{-3}, respectively. This is consistent with previous work for the U.S. East Coast showing that aerosol mass concentrations are highest in the summer due to some combination of enhanced photochemistry to generate secondary aerosol species, transported biomass burning emissions, high humidity to promote secondary aerosol formation, and stagnation events.[20,64] Also, this site tends to have shallower boundary layer heights in the summer months as compared to the spring, which helps also concentrate more pollutants in the narrow surface layer. Additionally, there is less precipitation accumulation in the summer, which reduces local aerosol removal *via* wet scavenging.[65] PM concentrations were lower and comparable for all months between September and May. The lowest $PM_{2.5}$ and PM_{10} values were 2.94 μg m^{-3} (December) and 4.65 μg m^{-3} (December), respectively.

The $PM_{2.5}:PM_{10}$ annual profile exhibits multiple modes with a peak in July (0.67) and another mode in the winter peaking in December (0.64). The lowest $PM_{2.5}:PM_{10}$ ratio was observed in June and September (0.53). For context,[63] reported that $PM_{2.5}:PM_{10}$ ratios below 0.35 typically correspond to local dust events, which are not expected in this region due to the landscape type being much different than a typical semi-arid/arid region with more dust surfaces. In contrast, Acadia NP likely gets dust influence from long-range transport. In their analysis of dust events across the U.S. East Coast,[22] reported the following mean $PM_{2.5}:PM_{10}$ ratios at Acadia NP for the following dust sources: 0.79 (African), 0.60 (Asian), 0.67 (Other), 0.65 (Mix). That same study examined 78 dust events affecting Acadia NP and found that 5 and 22 could be assigned to African and Asian sources, respectively, with 46 being Other (neither African or Asian) and 5 being Mix (African and Asian). Asian dust events are more common between March and June, whereas African dust affects Acadia NP more between June and August according to.[22] Thus, while other factors affect the $PM_{2.5}:PM_{10}$ aside from just dust, such as biomass burning, the values in Fig. 3 provide support for dust influence, especially between March and June. Comparing the $PM_{2.5}:PM_{10}$ profile to that of sea salt suggests that sea salt is likely not a key driver of reducing the $PM_{2.5}:PM_{10}$ ratio on the monthly scales examined in Fig. 3.

Next we look more closely at $PM_{2.5}$ in Fig. 3a by viewing the annual profile of RCFM components: ammonium nitrate, elemental carbon, sea salt, ammonium sulfate, organic mass, and fine soil. The most prominent components are organics and ammonium sulfate with maximum concentrations of 2.66 μg m^{-3} and 2.24 μg m^{-3}, respectively, in July. The concentrations of organics and ammonium sulfate generally increase in the summer months due at least partly to more secondary formation in conditions favoring more photochemistry (high temperature and solar radiation) and aqueous processing (enhanced RH).[20,64,66] This is consistent with a past report of the highest annual ratios of SOA to $PM_{2.5}$ being between June and September.[26] Also highest between June–August is elemental carbon (peaking in July at 0.21 μg m^{-3}) due probably to biomass burning influence, which is known to impact the region in the summer.[23,24,67,68]

Fine soil levels vary between 0.10–0.27 μg m^{-3} throughout the year with its highest levels between March–August (0.19–

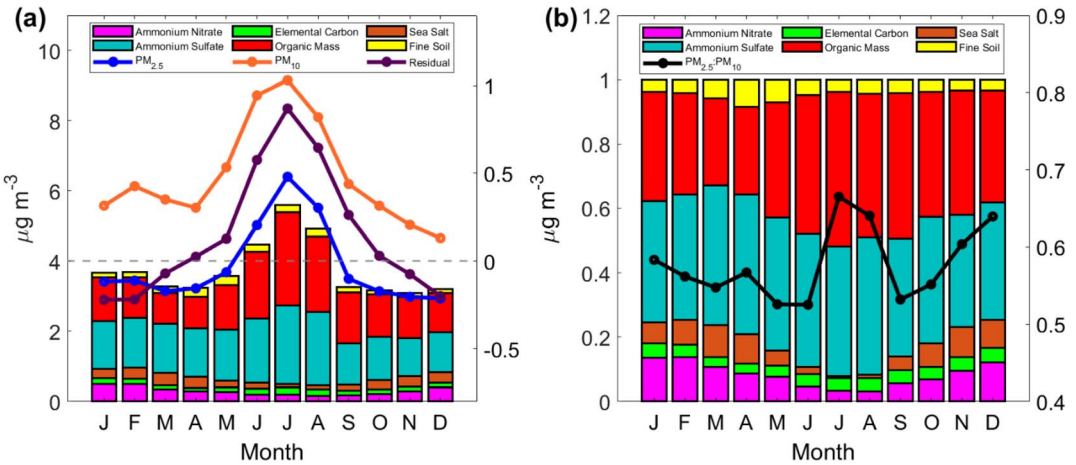

Fig. 3 Monthly averaged (a) mass concentrations of reconstructed $PM_{2.5}$ components, $PM_{2.5}$, and PM_{10}. Residual $PM_{2.5}$ is shown on the right *y*-axis. A dashed horizontal line for a residual mass of 0 μg m^{-3} is provided for context. (b) Monthly averaged $PM_{2.5}$ constituent mass fractions, with $PM_{2.5}:PM_{10}$ shown on the right axis. All results in this figure are based on IMPROVE data at Acadia NP from January 2001 to December 2021.

0.27 μg m^{-3}), which coincides with when the site is most influenced by long-range transport of Asian and African dust in addition to probable sources over North America.[22] Sea salt and ammonium nitrate differ from other RCFM components as they are lowest in the summer months and highest in the winter. Ammonium nitrate peaked between December–February (0.39–0.50 μg m^{-3}) whereas sea salt was highest from October till April (0.26–0.36 μg m^{-3}). Ammonium nitrate is semi-volatile and generally favors colder conditions in the study region.[69] Furthermore, findings from the 2015 Wintertime Investigation of Transport, Emissions, and Reactivity (WINTER) campaign revealed that low particle pH in winter also promotes nitrate partitioning to the particulate phase.[70] Sea salt can be affected by a number of variables, one of which is wind speed[71] that generally is lowest in summer consistent with lowest sea salt values. Past work has shown higher sea salt aerosol optical depth values over the northwest Atlantic for the winter season along with highest wind speeds.[20]

The $PM_{2.5}$ residual ($PM_{2.5}$-RCFM) was negative between November–March and ranged from −0.22 (January) to 0.87 (July). A past study reported that residual mass across the U.S. mostly changed from being negative prior to 2011 to being positive after 2011, with the highest residuals being in the summertime.[44] One of the reasons for the change was attributed to increased ratios of organic mass to organic carbon after 2011, with higher values reported over the eastern U.S.[72] during summer. Another study comparing measured $PM_{2.5}$ (*via* Federal Reference Method, FRM) *versus* sum of constituents *via* various filter-based and continuous measurements in Pittsburgh, Pennsylvania showed that volatilization losses affect FRM-based $PM_{2.5}$ mass measurements, which is especially important to consider in winter and also during periods of high organic and/or ammonium nitrate concentrations.[73] That study also showed that FRM-based $PM_{2.5}$ exceeded the sum of measured constituents during summer periods owing to retention of water on filters, especially during more acidic conditions. Those explanations along with adsorption of organic vapors on quartz filters were reported in another study too.[46] The seasonal differences and associated explanations related to residual mass explained in the literature seem consistent with what is observed in this study.

Fig. 3b shows the monthly profile of RCFM mass fractions to better visualize the relative importance of different species during the year. This panel shows more clearly the higher relative importance of fine soil during the typical spring time dust season[74] (March–May; mass fractions of 0.06–0.08), the dominance of secondarily formed species (ammonium sulfate and organic mass) in the summer (total mass fraction between both of ∼0.85–0.88 between June–August), the more pronounced importance of sea salt and ammonium nitrate outside of summer, and the relatively stable contribution of elemental carbon during the year.

Next, we look at how each $PM_{2.5}$ component, as well as overall $PM_{2.5}$, changes throughout the 21 year study period (Fig. 4). We caution that over the study period, there were some changes in the analytical methods used.[48] For instance, there was a change in thermal/optical carbon analyzers at the end of

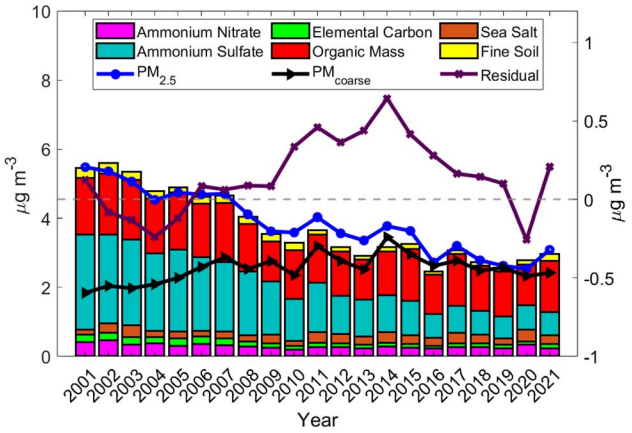

Fig. 4 Interannual variation in mass concentrations of reconstructed $PM_{2.5}$ components, $PM_{2.5}$, and PM_{coarse}, with the residual $PM_{2.5}$ shown on the right *y*-axis. Results are based on IMPROVE data at Acadia NP from January 2001 to December 2021.

2004 with potential implication for elemental carbon trend analysis.[75] The RCFM sum of $PM_{2.5}$ constituents decreased from 5.45 to 2.97 μg m^{-3} from January 2001 to December 2021, respectively. The component with the largest decrease is ammonium sulfate with a range of 2.11 μg m^{-3}, which is explained by well-documented regulatory activities to reduce SO_2 emissions across the U.S. and other regions.[76–79] Elemental carbon exhibits a decrease as well with mean annual values ranging from 0.18–0.22 μg m^{-3} between 2001 and 2007 in contrast to 0.08–0.14 μg m^{-3} beginning in 2008. This is also in line with regulatory activities, which have been especially important for major sources over the eastern U.S.[20,80] The other constituents did not exhibit any pronounced trend over the study duration, probably due to how some components are largely driven by natural emissions such as sea salt and fine soil. $PM_{2.5}$ generally followed the concentration sum of RCFM components and exhibited a maximum concentration in 2001 (5.48 μg m^{-3}) and a minimum value in 2020 (2.53 μg m^{-3}). PM_{coarse} was relatively stable throughout the years, whereas residual mass exhibited more pronounced positive values between 2009–2017 (0.08–0.64 μg m^{-3}) with the reason being uncertain and out of the scope of this work.

3.3 Concentration weighted trajectories

To understand the seasonally-dependent influence of atmospheric circulation on aerosol composition at Acadia NP, Fig. 5 shows concentration weighted trajectories dependent on surface $PM_{2.5}$ measurements at Acadia NP. Owing to the use of four-day trajectories, the areal domains are quite large encompassing large swaths of North America and extending over the Atlantic Ocean (Fig. S2†). As a result, we show a more zoomed in version of the relevant areas over the northeast U.S. in Fig. 5 with potentially influential cities labeled for context. The most important areas influencing high $PM_{2.5}$ are colored with the higher weighted concentrations (*i.e.*, yellow-red). Regardless of season, the transport corridors coincident with highest $PM_{2.5}$ were from the northwest to the southwest, consistent with past

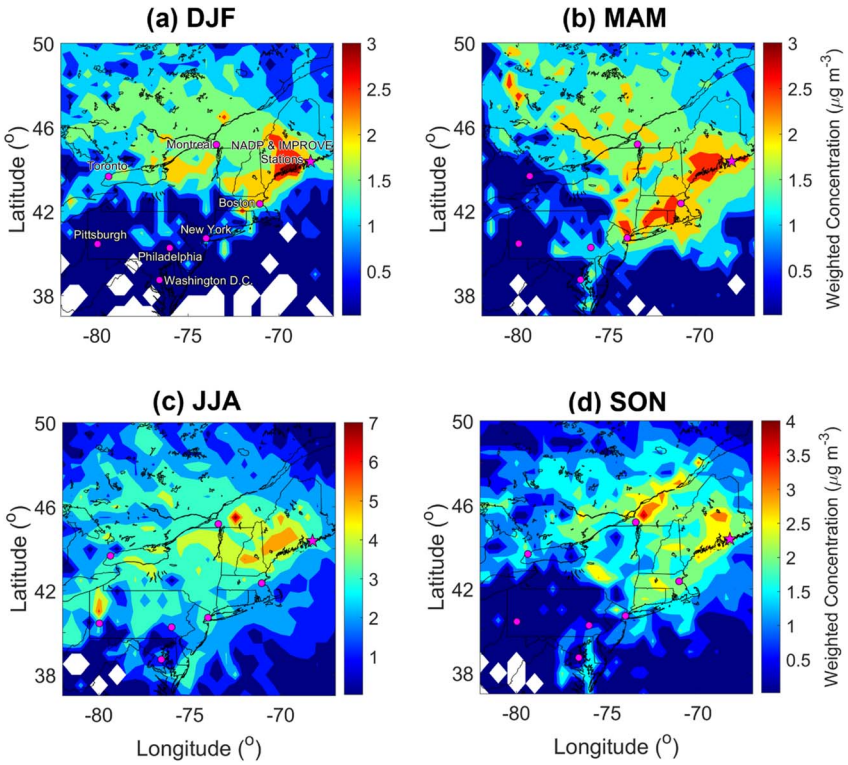

Fig. 5 Seasonal concentrated weighted trajectory profiles for $PM_{2.5}$ based on four-day back trajectories with ending altitude of 500 m AGL at Acadia National Park (pink star) between January 2017 and December 2021 for (a) December–February (DJF, winter), (b) March–May (MAM, spring), (c) June–August (JJA, summer), (d) September–November (SON, fall). Higher values (yellow-red) indicate that elevated $PM_{2.5}$ at Acadia NP was relatively more influenced by air traveling over those particular grid cells. Note the different color bar scales to better show variability within a particular season. Major cities are labeled in panel (a) with the same markers without labels in the other panels. A zoomed-out version of this figure is shown in Fig. S2.†

work,[27] suggestive of regional influence from (but not limited to) major cities such as New York, Boston (Massachusetts), Philadelphia/Pittsburgh (Pennsylvania), Washington D.C., and Montreal and Toronto in Canada. Influence from the west-northwest seems more prominent in all seasons except for summer for which there is relatively more influence from the southwest extending even beyond the southwest of Pittsburgh. The summer results also show influence from *trans*-Atlantic flow (Fig. S2†), consistent with the strengthening of the Bermuda-Azores high in summertime that promotes easterly trajectories south of approximately 25° N that curve and move northward along the U.S. East Coast; this wind pattern helps transport southeast U.S. emissions and even North African dust up to the northeast U.S.[2,20,22] Fig. 5 also suggests effects of recirculation of air in the form of onshore winds from the Atlantic Ocean as has been noted by others[81] based on pixels offshore with relatively high weighted $PM_{2.5}$ concentrations; this appears to be more prominent in the spring season.

3.4 Extreme $PM_{2.5}$ events

As mentioned in Section 2.6, each extreme $PM_{2.5}$ days (defined based on $PM_{2.5} \geq$ 98th percentile for a given month) is categorized as a sulfate, dust, and/or smoke event based on NAAPS data (Table 1). We caution that this definition does not mean the $PM_{2.5}$ levels are abnormally high relative to other regions; instead, they represent what is extreme relative to just this single site for a given month. This method follows past work.[53,58,82] Based on the criteria used for extreme events in the two subsets of years examined (2002–2006 and 2017–2021), sulfate corresponded to the most $PM_{2.5}$ extreme event days for both periods (17 out of 25 in 2002–2006 and 15 out of 27 in 2017–2021). An important difference between the subsets of years examined is that in the most recent period (2017–2021) the number of smoke events increased (12 *versus* 7 in 2002–2006) covering more months (March–December in 2017–2021) as compared to the earliest years (April–August in 2002–2006). This increase in smoke events as defined by criteria in our study is consistent with reports of more wildfires influencing U.S. air quality over time.[23,24,83,84] Sulfate events occurred 1–2 times each month in the two periods. The singular dust event occurred in November between 2002–2006, consistent with the generally low fine soil levels and large distance away from major deserts. Table 1 suggests that regional combustion emissions and secondary formation mechanisms contribute to the highest $PM_{2.5}$ days as sulfate is derived from SO_2 emissions and is secondarily produced efficiently with more photochemistry and high humidity.[20,64,66] Furthermore, the increase of smoke events in summertime is consistent with past work showing that summer months have influence from biomass burning

Table 1 Monthly classification of extreme $PM_{2.5}$ events ($PM_{2.5} \geq$ 98th percentile for a given month with threshold value in first row) into categories of aerosol types from January 2002 to December 2006 and January 2017 to December 2021 in Acadia NP. NAAPS data were used to assign each event as sulfate, dust, and/or smoke

	J	F	M	A	M	J	J	A	S	O	N	D	Total
2002–2006													
98th% $PM_{2.5}$ ($\mu g\ m^{-3}$)	10.68	10.32	9.45	11.86	11.82	23.36	24.01	27.54	11.28	12.51	9.84	10.90	10.68
Sulfate	2	1	1	1	2	1	2	2	1	1	1	2	17
Dust	0	0	0	0	0	0	0	0	0	0	1	0	1
Smoke	0	0	0	1	1	1	2	2	0	0	0	0	7
Total	2	1	1	2	3	2	4	4	1	1	2	2	25
2017–2021													
98th% $PM_{2.5}$ ($\mu g\ m^{-3}$)	6.10	6.43	4.85	6.89	6.30	7.96	15.46	8.30	6.32	6.14	6.72	5.56	6.10
Sulfate	1	1	2	1	2	1	1	1	1	2	1	1	15
Dust	0	0	0	0	0	0	0	0	0	0	0	0	0
Smoke	0	0	2	1	2	1	1	1	1	1	1	1	12
Total	1	1	4	2	4	2	2	2	2	3	2	2	27

emissions sourced from western parts of North America and also eastern parts of the U.S.[23]

Table 2 additionally shows the concentration and mass fraction statistics from the IMPROVE data for the different extreme event categories. The statistics incorporate data from all months for a given extreme event type. Smoke events exhibited the highest $PM_{2.5}$ regardless of which period was examined (2002–2006 = 27.56 $\mu g\ m^{-3}$; 2017–2021 = 8.53 $\mu g\ m^{-3}$), accounted for mainly by ammonium sulfate (16.55 $\mu g\ m^{-3}$; 46% of total $PM_{2.5}$) in the earlier years and by organic mass (3.84 $\mu g\ m^{-3}$; 65% of total $PM_{2.5}$) in the most recent years. There was only one dust extreme event identified with the important characteristic from IMPROVE that it exhibited the highest PM_{coarse} of all the extreme event categories (6.29 $\mu g\ m^{-3}$ *versus* 4.14–5.58 $\mu g\ m^{-3}$ for other categories). The sulfate extreme event days exhibited a median $PM_{2.5}$ level of 14.26 $\mu g\ m^{-3}$ (2002–2006) and 8.22 $\mu g\ m^{-3}$ (2017–2021) with a chemical make-up in sharp contrast between the two periods with ammonium sulfate accounting for more of the $PM_{2.5}$ in the earliest years (~57%) and organic mass accounting for more in the recent years (~42%).

3.5 Cold air outbreak events

Here we aim to compare aerosol composition on days with CAO conditions at the Acadia NP site (*i.e.*, a potential inflow air mass to CAO clouds as shown in Fig. 1) relative to days with non-CAO conditions. Fig. S3† shows box plots to summarize differences in meteorological variables (temperature, relative humidity, wind speed, and accumulated precipitation) for CAO and non-CAO days between December–March in 2016–2021; Table 3 reports median values, which we focus on here. The most significant difference was for temperature: median values of −8.57 °C (CAO) and −0.79 °C (non-CAO). RH was also considerably lower on CAO days (60.38% *versus* 78.71%). There were reductions on CAO days for wind speed (1.63 *versus* 2.63 $m\ s^{-1}$) and no difference in median precipitation accumulation for both CAO and non-CAO days (0 mm for both). The significantly reduced temperatures and drier conditions are consistent with recent airborne measurements during CAO days in the marine boundary layer over the northwest Atlantic.[85]

Fig. S4† shows boxplots comparing $PM_{2.5}$, PM_{coarse}, and mass concentrations and mass fractions of the RCFM components of $PM_{2.5}$ for CAO events *versus* non-CAO days whereas

Table 2 The median values of concentration ($\mu g\ m^{-3}$) and relative fraction (in that order) for the RCFM components of $PM_{2.5}$, along with $PM_{2.5}$ and PM_{coarse} values for the different extreme event types identified using NAAPS (see Table 1) from January 2002 to December 2006 and January 2017 to December 2021

	Extreme event type					
	Sulfate		Dust		Smoke	
	2002–2006	2017–2021	2002–2006	2017–2021	2002–2006	2017–2021
Ammonium nitrate	0.88/0.08	0.80/0.11	1.18/0.12	—/—	0.64/0.02	0.67/0.10
Ammonium sulfate	7.27/0.57	1.59/0.23	4.00/0.40	—/—	16.55/0.65	1.69/0.22
Elemental carbon	0.59/0.04	0.36/0.05	0.66/0.07	—/—	0.56/0.02	0.35/0.04
Organic mass	3.76/0.25	3.77/0.42	3.51/0.35	—/—	4.38/0.23	3.84/0.46
Sea salt	0.15/0.01	0.34/0.04	0.23/0.02	—/—	0.12/0.01	0.17/0.02
Fine soil	0.63/0.04	0.28/0.03	0.35/0.04	—/—	1.17/0.05	0.29/0.03
$PM_{2.5}$	14.26/—	8.22/—	10.20/—	—/—	27.56/—	8.53/—
PM_{coarse}	4.14/—	5.41/—	6.29/—	—/—	4.14/—	5.58/—

Table 3 Median values of meteorological variables and mass concentration (μg m^{-3}) and mass fraction values of each RCFM component of $PM_{2.5}$, along with $PM_{2.5}$ and coarse mass ($PM_{10} - PM_{2.5}$) for CAO and non-CAO days in December–March from 2016–2021. There were 26 and 153 CAO and non-CAO days in the analysis with IMPROVE data, and those are the days used for both the weather and aerosol results below

	CAO day	Non-CAO day
Temperature (°C)	−8.57	−0.79
Relative humidity (%)	60.38	78.71
Wind speed (m s^{-1})	1.63	2.63
Precipitation (mm)	0	0

	Concentration (μg m^{-3})		Mass fraction	
	CAO day	Non-CAO day	CAO day	Non-CAO day
Ammonium nitrate	0.23	0.25	0.12	0.12
Ammonium sulfate	0.53	0.74	0.32	0.30
Elemental carbon	0.08	0.08	0.04	0.04
Organic mass	0.74	0.83	0.38	0.37
Sea salt	0.14	0.17	0.06	0.07
Fine soil	0.13	0.08	0.06	0.03
$PM_{2.5}$	1.71	2.15	—	—
PM_{coarse}	1.74	1.70	—	—

Table 3 shows the median values. Composition variables revealed comparable levels for the two categories of days, with a few exceptions. The median value of ammonium sulfate on CAO days was 0.53 μg m^{-3} whereas the median value on non-CAO days was 0.74 μg m^{-3}. The next highest absolute value change was for organic matter, increasing from (CAO) 0.74 μg m^{-3} to (non-CAO) 0.83 μg m^{-3}. The only reduced median value on non-CAO days (albeit very slight) was for fine soil (0.13 *versus* 0.08 μg m^{-3}). $PM_{2.5}$ decreased on CAO days (1.71 *versus* 2.15 μg m^{-3}) whereas PM_{coarse} was slightly higher on CAO days (1.74 *versus* 1.70 μg m^{-3}).

As the motivation of this analysis is to characterize what the boundary layer aerosol characteristics are for air upstream of CAO cloud decks, it is useful to report that the mass composition is mostly governed by ammonium sulfate and organic matter (mass fractions of 0.32 and 0.38, respectively), followed by ammonium nitrate (0.12), sea salt and fine soil (both 0.06), and EC (0.04). Interestingly, the mass fractions of sulfate and organic mass from an Aerosol Mass Spectrometer (AMS) during airborne flights offshore the northeast U.S. (but farther south than Acadia NP) were approximately 0.45 and 0.34, respectively, during flight legs below cloud bases during CAO events.[86] That study's mass fractions of nitrate and ammonium were 0.07 and 0.13, respectively. Note though that the AMS focuses on the submicron aerosol fraction and cannot detect fine soil, sea salt, or elemental carbon. Generally speaking though, the mass fractions from IMPROVE *versus* the airborne measurements are comparable in light of the differences in variables compared and size ranges of the two respective datasets. It is expected that the aerosol composition could still change offshore and that measurements at Acadia NP are not a perfect representation of the CCN and IN composition in CAO cloud deck, especially if entrainment of free tropospheric aerosol becomes important for the boundary layer CCN budget farther offshore.[39] However, the changes are not expected to be too significant especially if they involve additional influence of ocean surface emissions, which suggests that the mass fraction of sea salt from IMPROVE represents a lower limit for the aerosol composition profile impacting the leading edges of offshore CAO clouds.

While the aerosol types quantified with IMPROVE measurements can serve as efficient CCN, especially so due to appreciable contributions from hygroscopic components (sulfate, nitrate, sea salt), less uncertain is what aerosol types can serve as efficient INPs. For context, one past study focusing on an Arctic CAO showed that INPs can include particles containing organic carbon and sea salt,[87] whereas another examining a CAO over the Norwegian and Barents Seas identified mineral dust mixed with biogenic materials as the predominant source of INPs.[15] Other works have pointed to glacial dust,[88,89] biological particles from both forests[90] and the ocean surface,[91,92] and thawing permafrost[93] as sources of INPs in the North Atlantic and Arctic regions. Certainly more research is warranted to better understand what aerosol types contribute most to the CCN and INP budgets offshore the northeast U.S. during CAOs. Our analysis is limited to mass-based units, so it is important to note that cloud droplet number concentrations are more sensitive to aerosol number concentrations. The results here can potentially aid modeling studies aiming to use the relative amounts of the species reported above to compute the hygroscopic properties of aerosol, which are needed in simulations of droplet activation over the northwest Atlantic.[17,38]

3.6 Wet deposition composition profile

Monthly average precipitation ion profiles are shown in Fig. 6, which differ considerably from the PM results in terms of annual patterns and relative importance of various species. Concentrations and mass fractions are shown for ammonium (NH_4^+), calcium (Ca^{2+}), sulfate (SO_4^{2-}), nitrate (NO_3^-), chloride (Cl^-), potassium (K^+), magnesium (Mg^{2+}), and sodium (Na^+). pH is additionally shown. Natural rainwater is reported to have

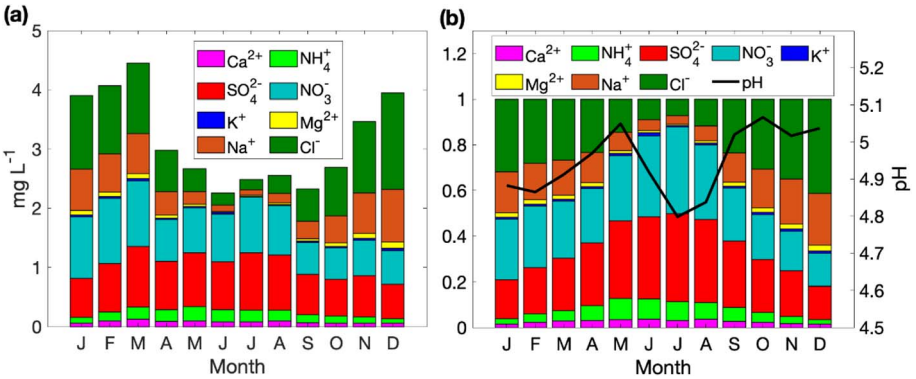

Fig. 6 Monthly average of (a) aqueous concentrations and (b) mass fractions of ions with pH on the right axis. These results are based on weekly NADP precipitation samples collected at Acadia NP from January 2001 to December 2021.

a pH of 5.6 [94] and decreases due to acidic ions from anthropogenic emissions, which has been well-documented for the northeastern U.S. in past decades.[95–97] The monthly average pH profile is bimodal (peaks in May and October) with values ranging from 4.8 (July) to 5.1 (October) and an annual mean pH of 4.95. Other work has shown the same type of bimodal profile for pH with peaks in late spring and fall for U.S. East Coast sites including in New Jersey and South Carolina.[98] The dip in acidity in the summer months coincides with the highest relative influence of the two acidic species, NO_3^- and SO_4^{2-}.

The monthly mass fraction profile was heavily influenced by Cl^- (0.22–0.41), NO_3^- (0.26–0.38), SO_4^{2-} (0.27–0.39), and Na^+ (0.13–0.27) (Fig. 6b). Cl^- and Na^+ are the two major sea salt constituents that contribute to precipitation *via* their role as either CCN or IN depending on the phase of the clouds producing the precipitation. Sea salt particles can be larger than 2.5 μm in diameter and they typically range from 0.01–10 μm,[99] with the majority of particles contributing to NADP samples presumably having a diameter larger than 2.5 μm due to mass concentration units used. This is largely why sea salt accounts for more of the mass fraction profile in wet deposition as compared to $PM_{2.5}$; furthermore, sea salt is very hygroscopic and one of the best types of CCN. A high concentration of Cl^- and Na^+ at a coastal site is a common trend along the East Coast because of the proximity to the Atlantic Ocean.[20] The pronounced influence of sea salt in wet deposition is why the total aqueous concentration was highest between November and March, which is consistent with IMPROVE data showing sea salt contributing the most mass generally in those months too albeit based on just measurements below 2.5 μm. It should be noted that SO_4^{2-}, Mg^{2+}, and K^+ are sea salt components too and thus their mass profiles are also influenced by sea salt throughout the year but especially between November and March.

The increase in SO_4^{2-}, NO_3^-, and NH_4^+ mass fractions in the summer months is most likely aided in part due to secondary formation mechanisms in the aerosol phase, which is linked to the NADP data because of the role of these particles in acting as CCN or being removed by precipitation below clouds. Although low in absolute mass contribution, Ca^{2+} exhibits relatively higher concentrations between March and August, which is consistent with the higher fine soil levels in those months too since Ca^{2+} is a tracer for soil dust.[100–102] The higher relative contribution of NO_3^- to wet deposition as compared to $PM_{2.5}$ is consistent with what has been observed at other sites across the U.S. East Coast[20] and also in central California.[33] This is probably because NO_3^- is associated with sea salt,[101,103,104] which was confirmed with past aerosol measurements at the nearby Appledore Island showing NO_3^- peaking in mass at ~4 μm with a secondary peak below 1 μm.[31]

Fig. 7 presents the average yearly aqueous concentrations from January 2001 to December 2021. pH generally increased over time from as low as 4.64 (2001, 2004) to as high as 5.23 (2020), which corresponds to the overall reductions in acids throughout the study period as demonstrated by SO_4^{2-} and NO_3^-. This is consistent with similar reports of increasing pH in wet deposition over the northeast U.S.,[105] including at Whiteface Mountain (New York).[106] The ion with the largest decrease is SO_4^{2-} with a range of 1.09 mg L^{-1} when comparing its maximum (1.44 mg L^{-1}) and minimum (0.35 mg L^{-1}) values in 2001 and 2019, respectively. The only other major reduction was for NO_3^-, with maximum and minimum values of 1.44 mg L^{-1} (2001) and 0.49 mg L^{-1} (2018), respectively. NH_4^+ tended to exhibit slightly higher values in the beginning portion of the study year with values between 2001 and 2009 ranging between 0.14–0.22 mg L^{-1} with a mean of 0.18 mg L^{-1}, whereas the period from 2010 and 2021 exhibited values between 0.13–0.19 mg L^{-1} with a mean of 0.15 mg L^{-1}. The other species did not exhibit any substantial interannual variations.

3.7 Interrelationships

3.7.1 NADP data. Comparing the relationships between the ions and pH of the precipitation provides more information on the precipitation chemistry at Acadia NP. Table 4 summarizes the interrelationships between each NADP species in the form of a correlation coefficient (r) matrix. Values shown are statistically significant at the 95% confidence level (*i.e.*, p-value <0.05) using a two-tailed Student's t-test. The strongest correlations are between sea salt constituents because of the high abundance of sea salt in the data and because sea salt is directly emitted without much change in its main components except for chloride depletion from reactions of salt with acidic species.[107]

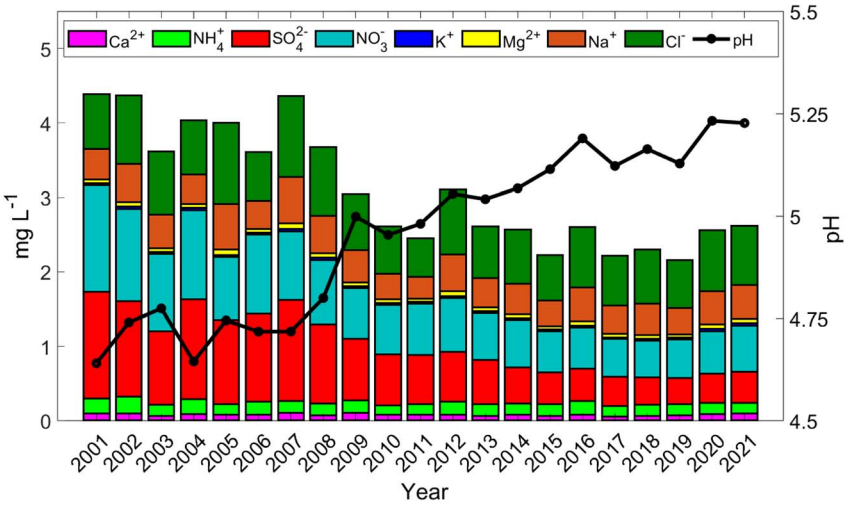

Fig. 7 Interannual variation in (left *y*-axis) aqueous concentrations of ions and (right *y*-axis) pH. Results are based on NADP data at Acadia NP from January 2001 to December 2021.

Table 4 Correlation matrix (*r* values) between various precipitation ion constituents detected in weekly NADP rain samples. Values shown are statistically significant (95%) using a two-tailed Student's *t*-test. The total number of points available in the study period is 1090

	Ca^{2+}	Mg^{2+}	K^+	Na^+	NH_4^+	NO_3^-	Cl^-	SO_4^{2-}	pH
Ca^{2+}	1.00								
Mg^{2+}	0.33	1.00							
K^+	0.48	0.77	1.00						
Na^+	0.21	0.99	0.72	1.00					
NH_4^+	0.69	0.07	0.26		1.00				
NO_3^-	0.67	0.11	0.22		0.74	1.00			
Cl^-	0.20	0.99	0.71	1.00			1.00		
SO_4^{2-}	0.53	0.23	0.29	0.17	0.71	0.70	0.16	1.00	
pH	−0.21				−0.35	−0.64		−0.71	1.00

Among the strongest relationships are the following: Mg^{2+} and Na^+ ($r = 0.99$), Mg^{2+} and Cl^- ($r = 0.99$), and Na^+ and Cl^- ($r = 1.00$). Strong but slighter weaker relationships for sea salt components were the following: Mg^{2+} and K^+ ($r = 0.77$) and Na^+ and K^+ ($r = 0.72$). pH exhibited significant correlations with just a subset of species (all negative), with strongest relationships being with the two acidic species known to reduce pH: NO_3^- ($r = -0.64$) and SO_4^{2-} ($r = -0.71$). Among non-sea salt species, strong correlations were observed for combinations of species known to make inorganic salts with one another as demonstrated by the RCFM results (*e.g.*, ammonium nitrate and ammonium sulfate): NH_4^+ and NO_3^- ($r = 0.74$) and NH_4^+ and SO_4^{2-} ($r = 0.71$). Another noteworthy relationship is between Ca^{2+} and NO_3^- ($r = 0.67$), which has been suggested in past studies to be due to their potential co-existence in dust aerosol.[35,98]

3.7.2 NADP *versus* IMPROVE data. Correlation results between IMPROVE and NADP data are discussed next (Table 5). Although not able to unambiguously point to any sort of causal relationship, interrelationships between variables can suggest potential aerosol–precipitation interactive effects worthy of future pursuit. In addition to common species between the two datasets, IMPROVE data for fine soil, organic carbon (OC), elemental carbon (EC), and coarse mass were included in the correlation analysis. Although we reference ions below, we note that ion chromatography was used in the IMPROVE dataset only to quantify sulfate, nitrate, and chloride whereas other species were detected *via* other techniques. While references are made below to statistically significant correlations, these assessments are based on a two-tailed Student's *t*-test and the correlations are still weak, which is due to the different nature of the datasets and associated factors that complicate direct associations.

In terms of correlations among individual species between themselves in the IMPROVE (I) and NADP (N) samples, the highest was for SO_4^{2-} ($r = 0.39$), followed by Ca^{2+} ($r = 0.29$), NO_3^- ($r = 0.25$), and Cl^- ($r = 0.17$). Dust's presence at Acadia NP is thought to be due to long-range transport, which could potentially increase the chance of a relationship between its surface aerosol and wet deposition levels if its vertical coverage was extensive. Fine soil (I) was best related to Ca^{2+} (N) among NADP variables, with the latter being a well-documented dust tracer species.[100,102,108,109] The correlation between those two variables was the highest among all interrelationships in Table 5, although still quite low as noted from the outset of this section. Fine soil (I) was also significantly correlated with NO_3^- (N) ($r = 0.22$) and SO_4^{2-} (N) ($r = 0.26$), which has been suggested in past work to point to a relationship between acids interacting and partitioning to dust particles that eventually impact clouds and precipitation.[34] Although the correlations for PM_{coarse} and NADP species were very weak based on *r* values, its highest one ($r = 0.11$) was with Ca^{2+} (N), which is at least consistent with there being a relationship between dust aerosol and wet deposition composition in the study region.

The sea salt constituents in NADP samples (*e.g.*, Cl^-, Na^+, Mg^{2+}) exhibited their strongest positive correlations with Cl^- in the IMPROVE dataset, followed by NO_3^-, Na^+, and then Mg^{2+}. This is consistent with sea salt particles being either effective

Table 5 Correlation matrix (*r* values) between precipitation ion species detected in NADP (N) samples and aerosol species detected in IMPROVE (I) samples. Values shown are statistically significant (95%) using a two-tailed Student's *t*-test. The total number of points available in the study period is 1090. Ion charges are only shows for those IMPROVE species analyzed *via* ion chromatography

	Ca (I)	Mg (I)	Na (I)	NO_3^- (I)	Cl^- (I)	K (I)	SO_4^{2-} (I)	Fine soil (I)	OC (I)	EC (I)	PM_{coarse} (I)
Ca^{2+} (N)	0.29			0.10		0.25	0.16	0.32	0.12	0.14	0.11
Mg^{2+} (N)	0.07	0.08	0.12	0.14	0.18	0.07			−0.14	−0.07	
Na^+ (N)		0.08	0.12	0.15	0.18			−0.09	−0.17	−0.08	−0.08
NO_3^- (N)	0.21			0.25		0.25	0.24	0.22	0.17	0.27	
Cl^- (N)		0.08	0.12	0.15	0.17			−0.09	−0.17	−0.08	−0.08
K^+ (N)	0.13		0.07	0.10	0.10	0.11		0.09			
SO_4^{2-} (N)	0.21	−0.07		0.14	−0.09	0.22	0.39	0.26	0.19	0.31	

CCN and/or being scavenged by precipitation. Organic and elemental carbon from the IMPROVE dataset were best correlated with NADP SO_4^{2-} and NO_3^-, which agrees with their general annual profiles showing highest values in the summertime.

4 Conclusions

This study examines air quality characteristics and relationships between aerosol wet deposition composition at a coastal site in Maine, U.S. (Acadia National Park). The results are important for public health and welfare, in addition to having implications for climate, ecosystem health, and aerosol–cloud interactions, especially with high interest in aerosol–cloud–meteorology interactions over the northwest Atlantic.[110] This site is downwind of several major populated cities in the eastern U.S. and eastern Canada, offering a chance to examine how this coastal site is impacted from such sources and also long-range transport.

The aerosol and wet deposition composition data behave differently during a typical year in terms of overall abundance and relative contributions of different species. $PM_{2.5}$ and PM_{10} are most abundant in the summer due to favorable meteorology and photochemistry promoting secondary formation of species like sulfate and organics, transported smoke, and reduced precipitation which could otherwise remove the aerosol. Aqueous concentrations of measured ions in wet deposition were conversely highest in the winter and aided in large part by sea salt which either seeded the droplets and/or was scavenged below clouds by falling drops. Regional emissions from the eastern U.S. and Canada were found to be especially influential for the extreme $PM_{2.5}$ events with high organic and ammonium sulfate levels. Long-range transport of smoke can affect the site especially in summer leading to the highest $PM_{2.5}$ levels of any aerosol extreme event type examined, whereas dust can also impact the site from potential sources like western North America, North Africa, and even Asia.[22] An important aspect of this work was to characterize the composition of aerosol along the coast during cold air outbreaks for which cloud decks develop offshore; there are very limited reports of aerosol composition of the CCN and IN impacting these cloud systems. Here we show that the aerosol is mainly comprised of sulfate-based salts and organics, and with more minor contributions from nitrate salts, sea salt, and elemental carbon.

The intercomparison between aerosol and wet deposition data afforded a chance to see what results emerge, even though limitations exist in such a comparison, with the goal of identifying potential relationships to pursue in future work. The correlations were expectedly not very high owing to differences between the nature of the two datasets, but noteworthy is that several individual species exhibited statistically significant correlations with themselves between aerosol and wet deposition samples: sulfate, calcium, nitrate, chloride. Also, there are significant relationships between dust and sea salt species between the two datasets, suggesting that these aerosol types are influential in aerosol–precipitation interactions.

This work helps advance understanding of air quality over the far northeast of the U.S. including a look at potential aerosol–precipitation interactions using IMPROVE and NADP datasets. The latter is a low-cost method of studying such relationships unlike costly airborne missions. A major limitation of the interrelationship analysis is that the aerosol data represent surface particulates whereas the wet deposition data represent processes impacting clouds farther aloft, which potentially had influence from other air masses. Also, the time resolution of the two datasets is coarse (daily for IMPROVE, weekly for NADP), which is another significant limitation. An improved study design would involve targeting precipitating clouds with vertically-resolved composition measurements at improved time resolution (*e.g.*, preferably <1 hour) from the surface to cloud level for trace gases, particles, and falling precipitation, in addition to cloud water in the clouds.

Interannual analysis of species concentrations revealed the success of regulatory actions in the U.S., with notable reductions in wet deposition levels of sulfate and nitrate that translated into increases in pH. These changes in pH can affect chemical reactions in droplets along with phase partitioning of semi-volatile gases. With reductions in $PM_{2.5}$ and ammonium sulfate over time, the relative importance of species other than sulfate have increased over the 21 year period examined. The changing mass fractions of species impacts particle optical and hygroscopic properties. The increasing relative importance of organics points to the importance of better understanding the chemical make-up of that subset of species, especially since different organic species may have different hygroscopic and

optical properties. Also, with changes in wildfire frequency and strength over North America,[111,112] this site will be affected more from such transported emissions.

With growing interest in aerosol–cloud interactions, especially over the northwest Atlantic Ocean due to its CAOs during winter months,[11,12,61] this study provides guidance on aerosol composition for air upwind of clouds forming during CAO days. Future efforts can investigate more closely the interactions between particles, clouds, and precipitation over the study region with the aid of airborne data combined with trajectory and chemical transport modeling as has been demonstrated by other past studies.[113] The use of radionuclide tracer species such as lead 210 in model simulations are particularly powerful for studying precipitation scavenging due to long half lives (22.3 years for ^{210}Pb), being primarily emitted from land, and attaching to particles with subsequent removal *via* wet scavenging.[114] An opportune dataset to allow for continued research into aerosol–precipitation interactions in the study region is that from the NASA ACTIVATE set of flights between 2020–2022 over the northwest Atlantic with detailed data for trace gases, aerosol particles, clouds/precipitation, and atmospheric state parameters.[110]

Data availability

IMPROVE data can be accessed at: **http://views.cira.colostate.edu/fed/**. NADP composition data can be accessed at: **https://nadp.slh.wisc.edu/networks/national-trends-network/**. Meteorological data for temperature, relativity humidity, wind speed, and solar radiation can be accessed at: **https://ard-request.air-resource.com/data.aspx**. Accumulated precipitation data can be accessed at: **https://views.cira.colostate.edu/fed/Pub/DatasetDetail.aspx?dsidse=5201**. MERRA-2 data can be accessed at: **https://disc.gsfc.nasa.gov/**. NAAPS data can be accessed at: **https://www.nrlmry.navy.mil/aerosol/**. NASA Worldview data can be accessed at: NASA Worldview **https://worldview.earthdata.nasa.gov**.

Author contributions

Data analysis was conducted by ASM and GB. Writing the original draft was performed by ASM and AS. All authors contributed in part to the discussion, review, and editing of the manuscript. All authors have given approval to the final version of the manuscript.

Conflicts of interest

There are no conflicts to declare.

Acknowledgements

Funding from this work was provided by NASA grant 80NSSC19K0442 in support of ACTIVATE, a NASA Earth Venture Suborbital-3 (EVS-3) investigation funded by NASA's Earth Science Division and managed through the Earth System Science Pathfinder Program Office. ASM additionally acknowledges support from the Scott Roberts scholarship to support undergraduate research from the University of Arizona's Department of Chemical and Environmental Engineering. The authors gratefully acknowledge the NOAA Air Resources Laboratory (ARL) for the provision of the HYSPLIT transport and dispersion model and READY website (**https://www.ready.noaa.gov**) used in this publication. The authors acknowledge the EPA Air Quality Systems (AQS) database (**https://www.epa.gov/aqs**). IMPROVE is a collaborative association of state, tribal, and federal agencies, and international partners. US Environmental Protection Agency is the primary funding source, with contracting and research support from the National Park Service. The Air Quality Group at the University of California, Davis is the central analytical laboratory, with ion analysis provided by Research Triangle Institute, and carbon analysis provided by Desert Research Institute.

References

1 A. Sorooshian, B. Anderson, S. E. Bauer, R. A. Braun, B. Cairns, E. Crosbie, H. Dadashazar, G. Diskin, R. Ferrare and R. C. Flagan, Aerosol–cloud–meteorology interaction airborne field investigations: Using lessons learned from the US West Coast in the design of ACTIVATE off the US East Coast, *Bull. Am. Meteorol. Soc.*, 2019, **100**, 1511–1528.

2 A. Sorooshian, A. F. Corral, R. A. Braun, B. Cairns, E. Crosbie, R. Ferrare, J. Hair, M. M. Kleb, A. Hossein Mardi and H. Maring, Atmospheric research over the western North Atlantic Ocean region and North American East Coast: A review of past work and challenges ahead, *J. Geophys. Res.:Atmos.*, 2020, **125**, e2019JD031626.

3 D. Painemal, A. F. Corral, A. Sorooshian, M. A. Brunke, S. Chellappan, V. Afzali Gorooh, S. H. Ham, L. O'Neill, W. L. Smith Jr and G. Tselioudis, An overview of atmospheric features over the Western North Atlantic Ocean and North American East Coast—Part 2: Circulation, boundary layer, and clouds, *J. Geophys. Res.:Atmos.*, 2021, **126**, e2020JD033423.

4 S. Kirschler, C. Voigt, B. Anderson, R. Campos Braga, G. Chen, A. F. Corral, E. Crosbie, H. Dadashazar, R. A. Ferrare and V. Hahn, Seasonal updraft speeds change cloud droplet number concentrations in low-level clouds over the western North Atlantic, *Atmos. Chem. Phys.*, 2022, **22**, 8299–8319.

5 E. Crosbie, L. D. Ziemba, M. A. Shook, T. Shingler, J. W. Hair, A. Sorooshian, R. A. Ferrare, B. Cairns, Y. Choi, J. DiGangi, G. S. Diskin, C. Hostetler, S. Kirschler, R. H. Moore, D. Painemal, C. Robinson, S. T. Seaman, K. L. Thornhill, C. Voigt and E. Winstead, Measurement report: Cloud and environmental properties associated with aggregated shallow marine cumulus and cumulus congestus, *Atmos. Chem. Phys.*, 2024, **24**, 6123–6152.

6 H. Dadashazar, D. Painemal, M. Alipanah, M. Brunke, S. Chellappan, A. F. Corral, E. Crosbie, S. Kirschler, H. Liu and R. H. Moore, Cloud drop number concentrations over

the western North Atlantic Ocean: seasonal cycle, aerosol interrelationships, and other influential factors, *Atmos. Chem. Phys.*, 2021, **21**, 10499–10526.

7 S. J. Abel, I. A. Boutle, K. Waite, S. Fox, P. R. Brown, R. Cotton, G. Lloyd, T. W. Choularton and K. N. Bower, The role of precipitation in controlling the transition from stratocumulus to cumulus clouds in a Northern Hemisphere cold-air outbreak, *J. Atmos. Sci.*, 2017, **74**, 2293–2314.

8 P. R. Field, R. Brožková, M. Chen, J. Dudhia, C. Lac, T. Hara, R. Honnert, J. Olson, P. Siebesma and S. de Roode, Exploring the convective grey zone with regional simulations of a cold air outbreak, *Q. J. R. Metereol. Soc.*, 2017, **143**, 2537–2555.

9 F. Pithan, G. Svensson, R. Caballero, D. Chechin, T. W. Cronin, A. M. Ekman, R. Neggers, M. D. Shupe, A. Solomon and M. Tjernström, Role of air-mass transformations in exchange between the Arctic and mid-latitudes, *Nat. Geosci.*, 2018, **11**, 805–812.

10 S. Melfi and S. P. Palm, Estimating the orientation and spacing of midlatitude linear convective boundary layer features: Cloud streets, *J. Atmos. Sci.*, 2012, **69**, 352–364.

11 F. Tornow, A. S. Ackerman and A. M. Fridlind, Preconditioning of overcast-to-broken cloud transitions by riming in marine cold air outbreaks, *Atmos. Chem. Phys.*, 2021, **21**, 12049–12067.

12 J. Chen, H. Wang, X. Li, D. Painemal, A. Sorooshian, K. L. Thornhill, C. Robinson and T. Shingler, Impact of Meteorological Factors on the Mesoscale Morphology of Cloud Streets during a Cold-Air Outbreak over the Western North Atlantic, *J. Atmos. Sci.*, 2022, **79**, 2863–2879.

13 B. Brümmer, Roll and Cell Convection in Wintertime Arctic Cold-Air Outbreaks, *J. Atmos. Sci.*, 1999, **56**, 2613–2636.

14 S. Chellappan, P. Zuidema, S. Kirschler, C. Voigt, B. Cairns, E. C. Crosbie, R. Ferrare, J. Hair, D. Painemal, T. Shingler, M. Shook, K. L. Thornhill, F. Tornow and A. Sorooshian, Microphysical Evolution in Mixed-Phase Midlatitude Marine Cold-Air Outbreaks, *J. Atmos. Sci.*, 2024, **81**, 1725–1747.

15 E. N. Raif, S. L. Barr, M. D. Tarn, J. B. McQuaid, M. I. Daily, S. J. Abel, P. A. Barrett, K. N. Bower, P. R. Field, K. S. Carslaw and B. J. Murray, *High Ice-Nucleating Particle Concentrations Associated with Arctic Haze in Springtime Cold-Air Outbreaks*, EGUsphere, 2024, vol. 2024, pp. 1–38.

16 D. Painemal, S. Chellappan, W. L. Smith Jr, D. Spangenberg, J. M. Park, A. Ackerman, J. Chen, E. Crosbie, R. Ferrare and J. Hair, Wintertime synoptic patterns of midlatitude boundary layer clouds over the western North Atlantic: Climatology and insights from in situ ACTIVATE observations, *J. Geophys. Res.:Atmos.*, 2023, **128**, e2022JD037725.

17 X.-Y. Li, H. Wang, J. Chen, S. Endo, S. Kirschler, C. Voigt, E. Crosbie, L. D. Ziemba, D. Painemal and B. Cairns, Large-Eddy Simulations of Marine Boundary Layer Clouds Associated with Cold-Air Outbreaks during the ACTIVATE Campaign. Part II: Aerosol–Meteorology–Cloud Interaction, *J. Atmos. Sci.*, 2023, **80**, 1025–1045.

18 X. Y. Li, H. Wang, M. W. Christensen, J. Chen, S. Tang, S. Kirschler, E. Crosbie, L. D. Ziemba, D. Painemal and A. F. Corral, Process Modeling of Aerosol-Cloud Interaction in Summertime Precipitating Shallow Cumulus Over the Western North Atlantic, *J. Geophys. Res.:Atmos.*, 2024, **129**, e2023JD039489.

19 N. Bellouin, J. Quaas, E. Gryspeerdt, S. Kinne, P. Stier, D. Watson-Parris, O. Boucher, K. S. Carslaw, M. Christensen and A. L. Daniau, Bounding global aerosol radiative forcing of climate change, *Rev. Geophys.*, 2020, **58**, e2019RG000660.

20 A. F. Corral, R. A. Braun, B. Cairns, V. A. Gorooh, H. Liu, L. Ma, A. H. Mardi, D. Painemal, S. Stamnes and B. Van Diedenhoven, An overview of atmospheric features over the western North Atlantic Ocean and North American East Coast–Part 1: Analysis of aerosols, gases, and wet deposition chemistry, *J. Geophys. Res.:Atmos.*, 2021, **126**, e2020JD032592.

21 Y. Zhang, G. Luo and F. Yu, Seasonal Variations and Long-Term Trend of Dust Particle Number Concentration Over the Northeastern United States, *J. Geophys. Res.:Atmos.*, 2019, **124**, 13140–13155.

22 A. M. Aldhaif, D. H. Lopez, H. Dadashazar and A. Sorooshian, Sources, frequency, and chemical nature of dust events impacting the United States East Coast, *Atmos. Environ.*, 2020, **231**, 117456.

23 A. H. Mardi, H. Dadashazar, D. Painemal, T. Shingler, S. T. Seaman, M. A. Fenn, C. A. Hostetler and A. Sorooshian, Biomass Burning Over the United States East Coast and Western North Atlantic Ocean: Implications for Clouds and Air Quality, *J. Geophys. Res.:Atmos.*, 2021, **126**, e2021JD034916.

24 H. M. Rogers, J. C. Ditto and D. R. Gentner, Evidence for impacts on surface-level air quality in the northeastern US from long-distance transport of smoke from North American fires during the Long Island Sound Tropospheric Ozone Study (LISTOS) 2018, *Atmos. Chem. Phys.*, 2020, **20**, 671–682.

25 F. C. Fehsenfeld, G. Ancellet, T. S. Bates, A. Goldstein, R. Hardesty, R. Honrath, K. S. Law, A. Lewis, R. Leaitch and S. McKeen, International consortium for atmospheric research on transport and transformation (ICARTT): North America to Europe—Overview of the 2004 summer field study, *J. Geophys. Res.:Atmos.*, 2006, **111**, D23S01.

26 H. Liao, D. K. Henze, J. H. Seinfeld, S. Wu and L. J. Mickley, Biogenic secondary organic aerosol over the United States: Comparison of climatological simulations with observations, *J. Geophys. Res.:Atmos.*, 2007, **112**, D06201.

27 B. D. Keim, L. D. Meeker and J. F. Slater, Manual synoptic climate classification for the East Coast of New England (USA) with an application to PM2. 5 concentration, *Clim. Res.*, 2005, **28**, 143–153.

28 P. Quinn, T. Bates, D. Coffman, T. Onasch, D. Worsnop, T. Baynard, J. De Gouw, P. Goldan, W. Kuster and E. Williams, Impacts of sources and aging on submicrometer aerosol properties in the marine boundary

layer across the Gulf of Maine, *J. Geophys. Res.:Atmos.*, 2006, **111**, D23S36.
29 T. Bates, P. Quinn, D. Coffman, J. Johnson and A. Middlebrook, Dominance of organic aerosols in the marine boundary layer over the Gulf of Maine during NEAQS 2002 and their role in aerosol light scattering, *J. Geophys. Res.:Atmos.*, 2005, **110**, D18202.
30 W. C. Keene, J. Stutz, A. A. Pszenny, J. R. Maben, E. V. Fischer, A. M. Smith, R. von Glasow, S. Pechtl, B. C. Sive and R. K. Varner, Inorganic chlorine and bromine in coastal New England air during summer, *J. Geophys. Res.:Atmos.*, 2007, **112**, D10S12.
31 E. Fischer, A. Pszenny, W. Keene, J. Maben, A. Smith, A. Stohl and R. Talbot, Nitric acid phase partitioning and cycling in the New England coastal atmosphere, *J. Geophys. Res.:Atmos.*, 2006, **111**, D23S09.
32 A. M. Smith, W. C. Keene, J. R. Maben, A. A. Pszenny, E. Fischer and A. Stohl, Ammonia sources, transport, transformation, and deposition in coastal New England during summer, *J. Geophys. Res.:Atmos.*, 2007, **112**, D10S08.
33 H. Dadashazar, L. Ma and A. Sorooshian, Sources of pollution and interrelationships between aerosol and precipitation chemistry at a central California site, *Sci. Total Environ.*, 2019, **651**, 1776–1787.
34 A. F. Corral, H. Dadashazar, C. Stahl, E.-L. Edwards, P. Zuidema and A. Sorooshian, Source apportionment of aerosol at a coastal site and relationships with precipitation chemistry: A case study over the Southeast United States, *Atmosphere*, 2020, **11**, 1212.
35 A. Sorooshian, T. Shingler, A. Harpold, C. Feagles, T. Meixner and P. Brooks, Aerosol and precipitation chemistry in the southwestern United States: spatiotemporal trends and interrelationships, *Atmos. Chem. Phys.*, 2013, **13**, 7361–7379.
36 X.-Y. Li, H. Wang, J. Chen, S. Endo, G. George, B. Cairns, S. Chellappan, X. Zeng, S. Kirschler, C. Voigt, A. Sorooshian, E. Crosbie, G. Chen, R. A. Ferrare, W. I. Gustafson, J. W. Hair, M. M. Kleb, H. Liu, R. Moore, D. Painemal, C. Robinson, A. J. Scarino, M. Shook, T. J. Shingler, K. L. Thornhill, F. Tornow, H. Xiao, L. D. Ziemba and P. Zuidema, Large-Eddy Simulations of Marine Boundary Layer Clouds Associated with Cold-Air Outbreaks during the ACTIVATE Campaign. Part I: Case Setup and Sensitivities to Large-Scale Forcings, *J. Atmos. Sci.*, 2022, **79**, 73–100.
37 X.-Y. Li, H. Wang, J. Chen, S. Endo, S. Kirschler, C. Voigt, E. Crosbie, L. D. Ziemba, D. Painemal, B. Cairns, J. W. Hair, A. F. Corral, C. Robinson, H. Dadashazar, A. Sorooshian, G. Chen, R. A. Ferrare, M. M. Kleb, H. Liu, R. Moore, A. J. Scarino, M. A. Shook, T. J. Shingler, K. L. Thornhill, F. Tornow, H. Xiao and X. Zeng, Large-Eddy Simulations of Marine Boundary Layer Clouds Associated with Cold-Air Outbreaks during the ACTIVATE Campaign. Part II: Aerosol–Meteorology–Cloud Interaction, *J. Atmos. Sci.*, 2023, **80**, 1025–1045.
38 F. Tornow, A. S. Ackerman and A. M. Fridlind, Preconditioning of overcast-to-broken cloud transitions by riming in marine cold air outbreaks, *Atmos. Chem. Phys.*, 2021, **21**, 12049–12067.
39 F. Tornow, A. S. Ackerman, A. M. Fridlind, B. Cairns, E. C. Crosbie, S. Kirschler, R. H. Moore, D. Painemal, C. E. Robinson, C. Seethala, M. A. Shook, C. Voigt, E. L. Winstead, L. D. Ziemba, P. Zuidema and A. Sorooshian, Dilution of Boundary Layer Cloud Condensation Nucleus Concentrations by Free Tropospheric Entrainment During Marine Cold Air Outbreaks, *Geophys. Res. Lett.*, 2022, **49**, e2022GL098444.
40 F. Tornow, A. S. Ackerman, A. M. Fridlind, G. Tselioudis, B. Cairns, D. Painemal and G. Elsaesser, On the impact of a dry intrusion driving cloud-regime transitions in a midlatitude cold-air outbreak, *J. Atmos. Sci.*, 2023, **80**, 2881–2896.
41 U. S. Census, QuickFacts Hancock County, Maine, **https://www.census.gov/quickfacts/fact/table/hancockcountymaine/PST045223**, accessed 13 February 2024.
42 NPS, Acadia National Park Maine, **https://www.nps.gov/acad/traffic.htm#:~:text=During peakvisitorseasonat,tofillearlyeachday**, accessed 13 February 2024.
43 W. C. Malm, J. F. Sisler, D. Huffman, R. A. Eldred and T. A. Cahill, Spatial and seasonal trends in particle concentration and optical extinction in the United States, *J. Geophys. Res.:Atmos.*, 1994, **99**, 1347–1370.
44 J. L. Hand, A. J. Prenni, B. A. Schichtel, W. C. Malm and J. C. Chow, Trends in remote PM2. 5 residual mass across the United States: Implications for aerosol mass reconstruction in the IMPROVE network, *Atmos. Environ.*, 2019, **203**, 141–152.
45 J. L. Hand, T. E. Gill and B. A. Schichtel, Spatial and seasonal variability in fine mineral dust and coarse aerosol mass at remote sites across the United States, *J. Geophys. Res.:Atmos.*, 2017, **122**, 3080–3097.
46 J. C. Chow, D. H. Lowenthal, L.-W. A. Chen, X. Wang and J. G. Watson, Mass reconstruction methods for PM 2.5: a review, *Air Qual., Atmos. Health*, 2015, **8**, 243–263.
47 J. Hand, B. Schichtel, M. Pitchford, W. Malm and N. Frank, Seasonal composition of remote and urban fine particulate matter in the United States, *J. Geophys. Res.:Atmos.*, 2012, **117**, D05209.
48 J. L. Hand, IMPROVE Data User Guide 2023 (Version 2), 2023, **https://vista.cira.colostate.edu/Improve/data-user-guide/**.
49 R. Gelaro, W. McCarty, M. J. Suárez, R. Todling, A. Molod, L. Takacs, C. A. Randles, A. Darmenov, M. G. Bosilovich, R. Reichle, K. Wargan, L. Coy, R. Cullather, C. Draper, S. Akella, V. Buchard, A. Conaty, A. M. da Silva, W. Gu, G.-K. Kim, R. Koster, R. Lucchesi, D. Merkova, J. E. Nielsen, G. Partyka, S. Pawson, W. Putman, M. Rienecker, S. D. Schubert, M. Sienkiewicz and B. Zhao, The Modern-Era Retrospective Analysis for Research and Applications, Version 2 (MERRA-2), *J. Clim.*, 2017, **30**, 5419–5454.

50 G. Rolph, A. Stein and B. Stunder, Real-time environmental applications and display system: READY, *Environ. Model. Software*, 2017, **95**, 210–228.
51 A. F. Stein, R. R. Draxler, G. D. Rolph, B. J. Stunder, M. D. Cohen and F. Ngan, NOAA's HYSPLIT atmospheric transport and dispersion modeling system, *Bull. Am. Meteorol. Soc.*, 2015, **96**, 2059–2077.
52 G. Betito, A. Arellano and A. Sorooshian, Influence of Transboundary Pollution on the Variability of Surface Ozone Concentrations in the Desert Southwest of the US: Case Study for Arizona, *Atmosphere*, 2024, **15**, 401.
53 M. E. Gonzalez, J. G. Garfield, A. F. Corral, E.-L. Edwards, K. Zeider and A. Sorooshian, Extreme Aerosol Events at Mesa Verde, Colorado: Implications for Air Quality Management, *Atmosphere*, 2021, **12**, 1140.
54 M. R. A. Hilario, M. T. Cruz, P. A. Bañaga, G. Betito, R. A. Braun, C. Stahl, M. O. Cambaliza, G. R. Lorenzo, A. B. MacDonald and M. AzadiAghdam, Characterizing weekly cycles of particulate matter in a coastal megacity: The importance of a seasonal, size-resolved, and chemically speciated analysis, *J. Geophys. Res.:Atmos.*, 2020, **125**, e2020JD032614.
55 E. Crosbie, A. Sorooshian, N. A. Monfared, T. Shingler and O. Esmaili, A multi-year aerosol characterization for the greater Tehran area using satellite, surface, and modeling data, *Atmosphere*, 2014, **5**, 178–197.
56 K. Dimitriou, E. Remoundaki, E. Mantas and P. Kassomenos, Spatial distribution of source areas of PM2. 5 by Concentration Weighted Trajectory (CWT) model applied in PM2. 5 concentration and composition data, *Atmos. Environ.*, 2015, **116**, 138–145.
57 Y.-K. Hsu, T. M. Holsen and P. K. Hopke, Comparison of hybrid receptor models to locate PCB sources in Chicago, *Atmos. Environ.*, 2003, **37**, 545–562.
58 D. H. Lopez, M. R. Rabbani, E. Crosbie, A. Raman, A. F. Arellano and A. Sorooshian, Frequency and Character of Extreme Aerosol Events in the Southwestern United States: A Case Study Analysis in Arizona, *Atmosphere*, 2016, **7**, 1.
59 P. Lynch, J. S. Reid, D. L. Westphal, J. Zhang, T. F. Hogan, E. J. Hyer, C. A. Curtis, D. A. Hegg, Y. Shi and J. R. Campbell, An 11-year global gridded aerosol optical thickness reanalysis (v1. 0) for atmospheric and climate sciences, *Geosci. Model Dev.*, 2016, **9**, 1489–1522.
60 A. F. Corral, Y. Choi, E. Crosbie, H. Dadashazar, J. P. DiGangi, G. S. Diskin, M. Fenn, D. B. Harper, S. Kirschler and H. Liu, Cold Air Outbreaks Promote New Particle Formation Off the US East Coast, *Geophys. Res. Lett.*, 2022, **49**, e2021GL096073.
61 X.-Y. Li, H. Wang, J. Chen, S. Endo, G. George, B. Cairns, S. Chellappan, X. Zeng, S. Kirschler and C. Voigt, Large-eddy simulations of marine boundary layer clouds associated with cold-air outbreaks during the ACTIVATE campaign. Part I: Case setup and sensitivities to large-scale forcings, *J. Atmos. Sci.*, 2022, **79**, 73–100.
62 H. Ahmady-Birgani, P. Ravan, J. Simon Schlosser, A. Cuevas-Robles, M. AzadiAghdam and A. Sorooshian, Is there a relationship between Lake Urmia saline lakebed emissions and wet deposition composition in the Caucasus region?, *ACS Earth Space Chem.*, 2021, **5**, 2970–2985.
63 D. Tong, M. Dan, T. Wang and P. Lee, Long-term dust climatology in the western United States reconstructed from routine aerosol ground monitoring, *Atmos. Chem. Phys.*, 2012, **12**, 5189–5205.
64 A. P. Tai, L. J. Mickley and D. J. Jacob, Correlations between fine particulate matter (PM2.5) and meteorological variables in the United States: Implications for the sensitivity of PM2.5 to climate change, *Atmos. Environ.*, 2010, **44**, 3976–3984.
65 J. H. Seinfeld and S. N. Pandis, *Atmospheric Chemistry and Physics: From Air Pollution to Climate Change*, John Wiley & Sons, 2016.
66 Y. Gu, R. J. Huang, J. Duan, W. Xu, C. Lin, H. Zhong, Y. Wang, H. Ni, Q. Liu, R. Xu, L. Wang and Y. J. Li, Multiple pathways for the formation of secondary organic aerosol in the North China Plain in summer, *Atmos. Chem. Phys.*, 2023, **23**, 5419–5433.
67 L. J. DeBell, R. W. Talbot, J. E. Dibb, J. W. Munger, E. V. Fischer and S. E. Frolking, A major regional air pollution event in the northeastern United States caused by extensive forest fires in Quebec, Canada, *J. Geophys. Res.:Atmos.*, 2004, **109**, D19305.
68 J. Dreessen, J. Sullivan and R. Delgado, Observations and impacts of transported Canadian wildfire smoke on ozone and aerosol air quality in the Maryland region on June 9–12, 2015, *J. Air Waste Manage. Assoc.*, 2016, **66**, 842–862.
69 A. F. Corral, Y. Choi, B. L. Collister, E. Crosbie, H. Dadashazar, J. P. DiGangi, G. S. Diskin, M. Fenn, S. Kirschler and R. H. Moore, Dimethylamine in cloud water: a case study over the northwest Atlantic Ocean, *Environ. Sci.: Atmos.*, 2022, **2**, 1534–1550.
70 V. Shah, L. Jaeglé, J. A. Thornton, F. D. Lopez-Hilfiker, B. H. Lee, J. C. Schroder, P. Campuzano-Jost, J. L. Jimenez, H. Guo and A. P. Sullivan, Chemical feedbacks weaken the wintertime response of particulate sulfate and nitrate to emissions reductions over the eastern United States, *Proc. Natl. Acad. Sci. U. S. A.*, 2018, **115**, 8110–8115.
71 D. Erickson, J. Merrill and R. Duce, Seasonal estimates of global atmospheric sea-salt distributions, *J. Geophys. Res.:Atmos.*, 1986, **91**, 1067–1072.
72 W. Malm, B. Schichtel, J. Hand and A. Prenni, Implications of organic mass to carbon ratios increasing over time in the rural United States, *J. Geophys. Res.:Atmos.*, 2020, **125**, e2019JD031480.
73 S. L. Rees, A. L. Robinson, A. Khlystov, C. O. Stanier and S. N. Pandis, Mass balance closure and the Federal Reference Method for PM2.5 in Pittsburgh, Pennsylvania, *Atmos. Environ.*, 2004, **38**, 3305–3318.
74 J. L. Hand, W. H. White, K. A. Gebhart, N. P. Hyslop, T. E. Gill and B. A. Schichtel, Earlier onset of the spring fine dust season in the southwestern United States, *Geophys. Res. Lett.*, 2016, **43**, 4001–4009.

75 J. C. Chow, J. G. Watson, L. W. Chen, M. C. Chang, N. F. Robinson, D. Trimble and S. Kohl, The IMPROVE_A temperature protocol for thermal/optical carbon analysis: maintaining consistency with a long-term database, *J. Air Waste Manage. Assoc.*, 2007, **57**, 1014–1023.
76 J. Hand, B. Schichtel, W. Malm and M. Pitchford, Particulate sulfate ion concentration and SO2 emission trends in the United States from the early 1990s through 2010, *Atmos. Chem. Phys.*, 2012, **12**, 10353–10365.
77 J. Feng, E. Chan and R. Vet, Air quality in the eastern United States and Eastern Canada for 1990–2015: 25 years of change in response to emission reductions of SO2 and NOx in the region, *Atmos. Chem. Phys.*, 2020, **20**, 3107–3134.
78 S. J. Smith, H. Pitcher and T. M. Wigley, Global and regional anthropogenic sulfur dioxide emissions, *Global Planet. Change*, 2001, **29**, 99–119.
79 W. Keene, J. Moody, J. Galloway, J. Prospero, O. Cooper, S. Eckhardt and J. Maben, Long-term trends in aerosol and precipitation composition over the western North Atlantic Ocean at Bermuda, *Atmos. Chem. Phys.*, 2014, **14**, 8119–8135.
80 D. M. Murphy, J. C. Chow, E. M. Leibensperger, W. C. Malm, M. Pitchford, B. A. Schichtel, J. G. Watson and W. H. White, Decreases in elemental carbon and fine particle mass in the United States, *Atmos. Chem. Phys.*, 2011, **11**, 4679–4686.
81 S. Pechtl and R. von Glasow, Reactive chlorine in the marine boundary layer in the outflow of polluted continental air: A model study, *Geophys. Res. Lett.*, 2007, **34**, L11813.
82 A. M. Aldhaif, D. H. Lopez, H. Dadashazar, D. Painemal, A. J. Peters and A. Sorooshian, An aerosol climatology and implications for clouds at a remote marine site: Case study over Bermuda, *J. Geophys. Res.:Atmos.*, 2021, **126**, e2020JD034038.
83 R. Barbero, J. T. Abatzoglou, N. K. Larkin, C. A. Kolden and B. Stocks, Climate change presents increased potential for very large fires in the contiguous United States, *Int. J. Wildland Fire*, 2015, **24**, 892–899.
84 J. T. Abatzoglou and A. P. Williams, Impact of anthropogenic climate change on wildfire across western US forests, *Proc. Natl. Acad. Sci. U. S. A.*, 2016, **113**, 11770–11775.
85 R. Ferrare, J. Hair, C. Hostetler, T. Shingler, S. P. Burton, M. Fenn, M. Clayton, A. J. Scarino, D. Harper, S. Seaman, A. Cook, E. Crosbie, E. Winstead, L. Ziemba, L. Thornhill, C. Robinson, R. Moore, M. Vaughan, A. Sorooshian, J. S. Schlosser, H. Liu, B. Zhang, G. Diskin, J. DiGangi, J. Nowak, Y. Choi, P. Zuidema and S. Chellappan, Airborne HSRL-2 measurements of elevated aerosol depolarization associated with non-spherical sea salt, *Front. Remote Sens.*, 2023, **4**, DOI: **10.3389/frsen.2023.1143944**.
86 H. Dadashazar, A. F. Corral, E. Crosbie, S. Dmitrovic, S. Kirschler, K. McCauley, R. Moore, C. Robinson, J. S. Schlosser and M. Shook, Organic enrichment in droplet residual particles relative to out of cloud over the northwestern Atlantic: analysis of airborne ACTIVATE data, *Atmos. Chem. Phys.*, 2022, **22**, 13897–13913.
87 J. Inoue, Y. Tobo, F. Taketani and K. Sato, Oceanic Supply of Ice-Nucleating Particles and Its Effect on Ice Cloud Formation: A Case Study in the Arctic Ocean During a Cold-Air Outbreak in Early Winter, *Geophys. Res. Lett.*, 2021, **48**, e2021GL094646.
88 Y. Tobo, K. Adachi, P. J. DeMott, T. C. J. Hill, D. S. Hamilton, N. M. Mahowald, N. Nagatsuka, S. Ohata, J. Uetake, Y. Kondo and M. Koike, Glacially sourced dust as a potentially significant source of ice nucleating particles, *Nat. Geosci.*, 2019, **12**, 253–258.
89 A. Sanchez-Marroquin, O. Arnalds, K. J. Baustian-Dorsi, J. Browse, P. Dagsson-Waldhauserova, A. D. Harrison, E. C. Maters, K. J. Pringle, J. Vergara-Temprado, I. T. Burke, J. B. McQuaid, K. S. Carslaw and B. J. Murray, Iceland is an episodic source of atmospheric ice-nucleating particles relevant for mixed-phase clouds, *Sci. Adv.*, 2020, **6**, eaba8137.
90 J. Schneider, K. Höhler, P. Heikkilä, J. Keskinen, B. Bertozzi, P. Bogert, T. Schorr, N. S. Umo, F. Vogel, Z. Brasseur, Y. Wu, S. Hakala, J. Duplissy, D. Moisseev, M. Kulmala, M. P. Adams, B. J. Murray, K. Korhonen, L. Hao, E. S. Thomson, D. Castarède, T. Leisner, T. Petäjä and O. Möhler, The seasonal cycle of ice-nucleating particles linked to the abundance of biogenic aerosol in boreal forests, *Atmos. Chem. Phys.*, 2021, **21**, 3899–3918.
91 E. K. Bigg and C. Leck, Cloud-active particles over the central Arctic Ocean, *J. Geophys. Res.:Atmos.*, 2001, **106**, 32155–32166.
92 J. M. Creamean, J. N. Cross, R. Pickart, L. McRaven, P. Lin, A. Pacini, R. Hanlon, D. G. Schmale, J. Ceniceros, T. Aydell, N. Colombi, E. Bolger and P. J. DeMott, Ice Nucleating Particles Carried From Below a Phytoplankton Bloom to the Arctic Atmosphere, *Geophys. Res. Lett.*, 2019, **46**, 8572–8581.
93 J. M. Creamean, T. C. J. Hill, P. J. DeMott, J. Uetake, S. Kreidenweis and T. A. Douglas, Thawing permafrost: an overlooked source of seeds for Arctic cloud formation, *Environ. Res. Lett.*, 2020, **15**, 084022.
94 R. J. Charlson and H. Rodhe, Factors controlling the acidity of natural rainwater, *Nature*, 1982, **295**, 683–685.
95 J. N. Galloway, G. E. Likens and E. S. Edgerton, Acid Precipitation in the Northeastern United States: p H and Acidity, *Science*, 1976, **194**, 722–724.
96 G. E. Likens and F. H. Bormann, Acid rain: a serious regional environmental problem, *Science*, 1974, **184**, 1176–1179.
97 G. E. Likens, F. H. Bormann and N. M. Johnson, Acid rain, *Environ. Sci. Pol. Sustain. Dev.*, 1972, **14**, 33–40.
98 L. Ma, H. Dadashazar, M. R. A. Hilario, M. O. Cambaliza, G. R. Lorenzo, J. B. Simpas, P. Nguyen and A. Sorooshian, Contrasting wet deposition composition between three diverse islands and coastal North American sites, *Atmos. Environ.*, 2021, **244**, 117919.
99 M. Sofiev, J. Soares, M. Prank, G. de Leeuw and J. Kukkonen, A regional-to-global model of emission and transport of sea salt particles in the atmosphere, *J. Geophys. Res.:Atmos.*, 2011, **116**, D21302.

100 R. Arimoto, R. Duce, D. Savoie and J. Prospero, Trace elements in aerosol particles from Bermuda and Barbados: Concentrations, sources and relationships to aerosol sulfate, *J. Atmos. Chem.*, 1992, **14**, 439–457.

101 M. T. Cruz, P. A. Bañaga, P. A. Bañaga, G. Betito, R. A. Braun, C. Stahl, M. A. Aghdam, M. Obiminda Cambaliza, H. Dadashazar, M. R. Hilario, G. R. Lorenzo, L. Ma, A. B. MacDonald, P. C. Pabroa, J. R. Yee, J. B. Simpas and A. Sorooshian, Size-resolved composition and morphology of particulate matter during the southwest monsoon in Metro Manila, Philippines, *Atmos. Chem. Phys.*, 2019, **19**, 10675–10696.

102 D. R. Muhs, J. R. Budahn, J. M. Prospero, G. Skipp and S. R. Herwitz, Soil genesis on the island of Bermuda in the Quaternary: The importance of African dust transport and deposition, *J. Geophys. Res. Earth Surf.*, 2012, **117**, F03025.

103 R. A. Braun, H. Dadashazar, A. B. MacDonald, A. M. Aldhaif, L. C. Maudlin, E. Crosbie, M. A. Aghdam, A. Hossein Mardi and A. Sorooshian, Impact of wildfire emissions on chloride and bromide depletion in marine aerosol particles, *Environ. Sci. Technol.*, 2017, **51**, 9013–9021.

104 G. Prabhakar, B. Ervens, Z. Wang, L. Maudlin, M. Coggon, H. Jonsson, J. Seinfeld and A. Sorooshian, Sources of nitrate in stratocumulus cloud water: Airborne measurements during the 2011 E-PEACE and 2013 NiCE studies, *Atmos. Environ.*, 2014, **97**, 166–173.

105 H. O. T. Pye, A. Nenes, B. Alexander, A. P. Ault, M. C. Barth, S. L. Clegg, J. L. Collett Jr, K. M. Fahey, C. J. Hennigan, H. Herrmann, M. Kanakidou, J. T. Kelly, I. T. Ku, V. F. McNeill, N. Riemer, T. Schaefer, G. Shi, A. Tilgner, J. T. Walker, T. Wang, R. Weber, J. Xing, R. A. Zaveri and A. Zuend, The acidity of atmospheric particles and clouds, *Atmos. Chem. Phys.*, 2020, **20**, 4809–4888.

106 J. J. Schwab, P. Casson, R. Brandt, L. Husain, V. Dutkewicz, D. Wolfe, K. L. Demerjian, K. L. Civerolo, O. V. Rattigan, H. D. Felton and J. E. Dukett, Atmospheric Chemistry Measurements at Whiteface Mountain, NY: Cloud Water Chemistry, Precipitation Chemistry, and Particulate Matter, *Aerosol Air Qual. Res.*, 2016, **16**, 841–854.

107 E.-L. Edwards, Y. Choi, E. C. Crosbie, J. P. DiGangi, G. S. Diskin, C. E. Robinson, M. A. Shook, E. L. Winstead, L. D. Ziemba and A. Sorooshian, Sea salt reactivity over the northwest Atlantic: an in-depth look using the airborne ACTIVATE dataset, *Atmos. Chem. Phys.*, 2024, **24**, 3349–3378.

108 G. E. Shaw, Transport of Asian desert aerosol to the Hawaiian Islands, *J. Appl. Meteorol. Climatol.*, 1980, **19**, 1254–1259.

109 W. H. McDowell, C. G. Sánchez, C. E. Asbury and C. R. R. Pérez, Influence of sea salt aerosols and long range transport on precipitation chemistry at El Verde, Puerto Rico, *Atmos. Environ. Gen. Top*, 1990, **24**, 2813–2821.

110 A. Sorooshian, M. D. Alexandrov, A. D. Bell, R. Bennett, G. Betito, S. P. Burton, M. E. Buzanowicz, B. Cairns, E. V. Chemyakin, G. Chen, Y. Choi, B. L. Collister, A. L. Cook, A. F. Corral, E. C. Crosbie, B. van Diedenhoven, J. P. DiGangi, G. S. Diskin, S. Dmitrovic, E. L. Edwards, M. A. Fenn, R. A. Ferrare, D. van Gilst, J. W. Hair, D. B. Harper, M. R. A. Hilario, C. A. Hostetler, N. Jester, M. Jones, S. Kirschler, M. M. Kleb, J. M. Kusterer, S. Leavor, J. W. Lee, H. Liu, K. McCauley, R. H. Moore, J. Nied, A. Notari, J. B. Nowak, D. Painemal, K. E. Phillips, C. E. Robinson, A. J. Scarino, J. S. Schlosser, S. T. Seaman, C. Seethala, T. J. Shingler, M. A. Shook, K. A. Sinclair, W. L. Smith Jr, D. A. Spangenberg, S. A. Stamnes, K. L. Thornhill, C. Voigt, H. Vömel, A. P. Wasilewski, H. Wang, E. L. Winstead, K. Zeider, X. Zeng, B. Zhang, L. D. Ziemba and P. Zuidema, Spatially coordinated airborne data and complementary products for aerosol, gas, cloud, and meteorological studies: the NASA ACTIVATE dataset, *Earth Syst. Sci. Data*, 2023, **15**, 3419–3472.

111 J. K. Balch, B. A. Bradley, J. T. Abatzoglou, R. C. Nagy, E. J. Fusco and A. L. Mahood, Human-started wildfires expand the fire niche across the United States, *Proc. Natl. Acad. Sci. U. S. A.*, 2017, **114**, 2946–2951.

112 P. E. Dennison, S. C. Brewer, J. D. Arnold and M. A. Moritz, Large wildfire trends in the western United States, 1984–2011, *Geophys. Res. Lett.*, 2014, **41**, 2928–2933.

113 H. Liu, B. Zhang, R. H. Moore, L. D. Ziemba, R. A. Ferrare, H. Choi, A. Sorooshian, D. Painemal, H. Wang, M. A. Shook, A. J. Scarino, J. W. Hair, E. C. Crosbie, M. A. Fenn, T. J. Shingler, C. A. Hostetler, G. Chen, M. M. Kleb, G. Luo, F. Yu, J. L. Tackett, M. A. Vaughan, Y. Hu, G. S. Diskin, J. B. Nowak, J. P. DiGangi, Y. Choi, C. A. Keller and M. S. Johnson, *Tropospheric Aerosols over the Western North Atlantic Ocean during the Winter and Summer Campaigns of ACTIVATE 2020: Life Cycle, Transport, and Distribution*, EGUsphere, 2024, vol. 2024, pp. 1–68.

114 H. Dadashazar, M. Alipanah, M. R. A. Hilario, E. Crosbie, S. Kirschler, H. Liu, R. H. Moore, A. J. Peters, A. J. Scarino, M. Shook, K. L. Thornhill, C. Voigt, H. Wang, E. Winstead, B. Zhang, L. Ziemba and A. Sorooshian, Aerosol Responses to Precipitation Along North American Air Trajectories Arriving at Bermuda, *Atmos. Chem. Phys.*, 2021, 1–34, DOI: **10.5194/acp-2021-471**.